



IMAGE: A MAP OF THE STARS OF THE ORION CONSTELLATION

Print ISSN: 2631-8490 Online ISSN: 2631-8504

JournalPreview

London Journal of Research in Science: Natural and Formal
Volume 19 | Issue 2 | Compilation 1.0



JournalPreview

LONDON JOURNALS OF RESEARCH IN SCIENCE: NATURAL AND FORMAL

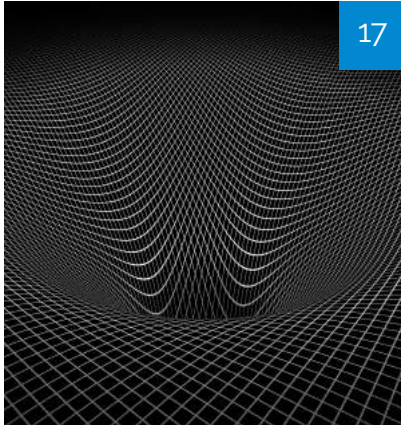
This document is a pre-published view of London Journal of Research in Science: Natural and Formal Volume 19, Issue 4 and Compilation 1.0. For any minor changes and updations kindly follow your paper's live editing URL given in sent email or get in touch with our support team at support@journalspress.com or visit our website to use live chat support. This is a beta document thus order, content or existence of papers may alter in the published eJournal. You are requested to kindly acknowledge and approve your research paper in this JournalPreview within three days.

Journal Content

In this Issue

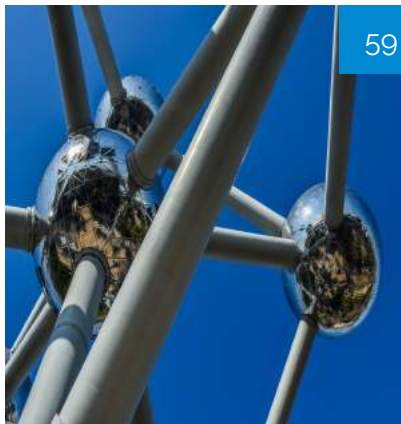


London
Journals Press



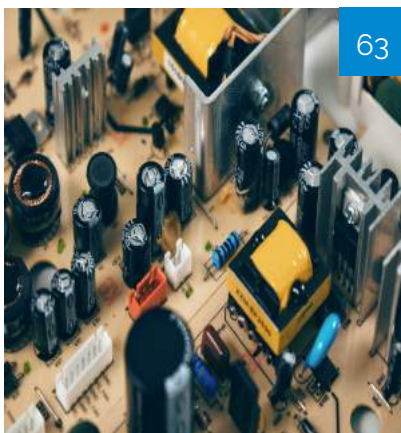
17

- i. Journal introduction and copyrights
 - ii. Featured blogs and online content
 - iii. Journal content
 - iv. Editorial Board Members
-



59

1. Artificial Neural Network based Artificial Intelligence Algorithms...
pg. 1-16
 2. Some Features of a Gravitational Field Quantization...
pg. 17-28
 3. Benefits of Precision Agriculture in Nigeria...
pg. 29-34
 4. Ion Potential Principle Summary
pg. 35-44
 5. Consortium Building among Academic Libraries...
pg. 45-52
 6. Fine-Structure Constant as Pure Geometric Number...
pg. 53-56
 7. Temperature Dependence of Static Dielectric Constant...
pg. 57-63
-



63

- v. London Journals Press Memberships



Scan to know paper details and
author's profile

Artificial Neural Network based Artificial Intelligent Algorithms for Accurate Monthly Load Forecasting of Power Consumption

Samuel Atuahene, Yukun Bao, Yao Yevenyo Ziggah & Patricia Semwaah Gyan

Huazhong University of Science and Technology

ABSTRACT

In this study, three artificial neural networks (ANN) techniques (backpropagation (BPNN), radial basis function network (RBFNN) and extreme learning machine (ELM)) were applied for accurate modeling and prediction of monthly load consumption. These models were trained for the first time on the data collected by the United State Energy Information Administration (USEIA) for five sectors from January 1973 to May 2017 (44 years). Performance evaluation of the methods was carried out using various statistical indicators including mean absolute percentage error (MAPE). The results revealed that the value of MAPE for BPNN which gave the optimum model for predicting the monthly load consumption were 0.999999885 and 0.999999069 for training and testing results respectively, ascertaining the accuracy and suitability of the model for monthly load consumption prediction.

Keywords: energy, load forecasting, back propagation neural network, radial basis function, extreme learning machine.

Classification: FOR code: 280212

Language: English



London
Journals Press

LJP Copyright ID: 925641
Print ISSN: 2631-8490
Online ISSN: 2631-8504

London Journal of Research in Science: Natural and Formal

Volume 19 | Issue 2 | Compilation 1.0



© 2019. Samuel Atuahene, Yukun Bao, Yao Yevenyo Ziggah & Patricia Semwaah Gyan. This is a research/review paper, distributed under the terms of the Creative Commons Attribution-Noncommercial 4.0 Unported License <http://creativecommons.org/licenses/by-nc/4.0/>), permitting all noncommercial use, distribution, and reproduction in any medium, provided the original work is properly cited.

Artificial Neural Network based Artificial Intelligent Algorithms for Accurate Monthly Load Forecasting of Power Consumption

Samuel Atuahene^α, Yukun Bao^σ, Yao Yevenyo Ziggah^ρ & Patricia Semwaah Gyan^ω

ABSTRACT

In this study, three artificial neural networks (ANN) techniques (backpropagation (BPNN), radial basis function network (RBFNN) and extreme learning machine (ELM)) were applied for accurate modeling and prediction of monthly load consumption. These models were trained for the first time on the data collected by the United State Energy Information Administration (USEIA) for five sectors from January 1973 to May 2017 (44 years). Performance evaluation of the methods was carried out using various statistical indicators including mean absolute percentage error (MAPE). The results revealed that the value of MAPE for BPNN which gave the optimum model for predicting the monthly load consumption were 0.999999885 and 0.999999069 for training and testing results respectively, ascertaining the accuracy and suitability of the model for monthly load consumption prediction.

Keywords: energy, load forecasting, back propagation neural network, radial basis function, extreme learning machine.

Author α σ: Center for Modern Information Management, School of Management Science and Engineering, Huazhong University of Science and Technology, Wuhan China.

ρ: Department of Geomatic Engineering, University of Mines and Technology, Tarkwa- Ghana.

ω: Faculty of Earth Resources, China University of Geosciences, Wuhan-China.

1. INTRODUCTION

Energy or load demand is the most useful entity in today's modern world. Monthly energy forecasting plays a vital role in the functioning efficiency of a power system, such as yearly hydro-thermal

maintenance scheduling, hydro-thermal coordination, unit commitment, demand side management, security assessment, interchange evaluation and others. Occasionally, we profligate electricity whiles other times quite careful about the usage of it. Yet, the objective is to make available an uninterrupted electricity supply to users. To arrive at this objective, there is the necessity for proper evaluation of present day and future consumption of power as well as the demand.

The large number of studies have compared the forecast accuracies of alternative models based on statistical theories. As a result, a technique which can predict the demand of consumers is needed as well as the actual capacity for generating power. In line with the, scholars have applied several estimation techniques to model and predict power consumption for commercial sectors, transport sectors [1], as well as electrical power sectors. These techniques are used by electricity companies to predict the amount of power needed to adequately supply the demand. Techniques for predicting power consumption uses a set of known entities to produce future values for the same or other entities. These predictive models can be categorized into two main approaches which are the classical and modern methods. The classical power consumption forecasting techniques such as stochastic time series and similar day look up approach have been the most widely applied methods by electrical companies [2]. Nevertheless, the classical methods becomes quite complicated when the actual historical energy consumption data does not support certain

statistical conditions [3]. Although they could be used in predicting power consumption, the advancement in mathematical sciences and technology have led to a paradigm shift in terms of power consumption prediction. Recently, artificial intelligent algorithms have been widely adopted by several scholars and have shown to produce better satisfactory results. This is because of its non-parametric and computational adaptiveness as compared to the classical which requires a fixed functional form (parametric) of the underlying data [4-13]. These studies main focus are to highlight the strength of the artificial intelligence methods and its compatibility to the classical power consumption techniques. Information gathered from these studies indicate that the artificial intelligent algorithms is the best predictor of load consumption.

Although a lot of research works have been done, this study provides for the first time a first-hand information, modelling and interpretation of the United State Energy Information Administration power consumption data for five different sectors from January 1973 to May 2017. Moreover, in spite of the reported merits of artificial intelligence techniques in the literature, applying and comparing multiple ANN techniques are yet to be explored. Hence, utilizing alternative techniques to predict power consumption for commercial sectors, transport sectors, as well as electrical power sectors has become essential. At this juncture, three ANN techniques of backpropagation, radial basis function and extreme learning machine have been used to analyze 533 months of data collected from January 1973 through to May 2017 to predict the amount of power needed to adequately supply the demand rise in the impending years.

As part of the main contributions of this study, an analytical perspective on the monthly energy demand was carried out based on the three ANN methods. Also, the developed models could be used by electrical power stations to predict the amount of power needed to adequately supply the demand. This paper has been divided as follows. The next section introduces a complete overview

of the three ANN models used and their training processes respectively. Section 3 discusses the theoretical concept of the ANN models. Section 4 introduces the output results and discussions of each of the models and section 5 presents the conclusions of the paper as well as indications of some direction for future works.

II. METHODOLOGY

The methodology used to develop the various ANN models are presented in the following sections.

2.1. Data Processing and Selection of Input Parameters

In this research, a total of 533 real load data from U.S Energy Information Administration from January 1973 through to May 2017 measured in trillion BTU for different sectors(US Energy Information Administration, 2016), were used in the BPNN, RBFNN and the ELM model formation. It is well-known that one of the contributing factors that affects the accuracy of the estimation of ANN is associated to the quality of datasets used to build the model and selecting of appropriate input parameters [14]. Hence, to ensure the quality of the data being used, a number of factors for instance, observation principles, observation techniques and period of observation as recommended by many researchers were taken into consideration [15]. Identification of our input parameters for the ANN training was the next step. It is well acknowledged here that, the input neuron acts as control variable with an influence on the desired output of the network. Therefore, the input data must serve as a representation of the condition for which training of the neural network is done [16].

2.2 Normalization of Data

In normal terms, the data to be processed are in different units' whiles having different physical meaning, therefore there is the need to normalize the data. Data normalization also help improve the convergence speed as well as reducing the chances of getting stuck in local minima.

Normalization will make sure the constant variability in the ANN model and to do so, the data set is mostly normalized to either [-1,1] or [0,1] while other times in other scaling criterion. In this research, we normalize the input and output selected variables in the interval of [-1,1] we the expression indicated in Eq. (1) as:

$$X_{normalized(0,1)} = \frac{X_{current} - X_{min}}{X_{max} - X_{min}} \quad (1)$$

Where $X_{normalized}$ represents the normalized data, $X_{current}$ is the data measured and X_{min} and X_{max} represents the minimum and maximum values of the measured coordinates. The resulted value will not go beyond 1 or get lower than 0, this method can be used only if we want to set a value in range [0, 1]. If we want to normalize our data in range [-1, 1] we can make 0 centralized as Eq. (2) depicts:

$$X_{normalized(0,1)} = \frac{X_{current} - ((X_{max} + X_{min}) / 2)}{(X_{max} - X_{min}) / 2} \quad (2)$$

2.3. Network Training

It must also be taken into consideration that datasets are trained in neural networks generating the required preferred output for particular inputs. Similarly, in this research, the objective is to train the neural networks to find an approximation of the functional relation between the output layer and the input layer. Therefore, 320 points were selected out of the 533 data point measurement as reference points sent $K = (K_1, K_2, K_3, \dots, K_{320})$ and employed as the set for training. It should be noted that, the data from January 1973 to August 1999 were selected as the training datasets. The remaining 213 points from September 1999 to May 2017 data points were used as the test set $T = (T_1, T_2, T_3, \dots, T_{213})$. In order to reduce the error function, the training set served as weight adjustment providing an unbiased estimation of the generalized error. During the network training, the BPNN was trained using the Levenberg-Marquardt

backpropagation algorithm. Gradient decent rule was employed for training the RBFNN while sigmoidal activation function was used to train the ELM. Training of the three network methods (BPNN, RBFNN and ELM) continued to train until no additional effective improvement occurred. Due to this reason, if there was a significant change in terms of error on the training results, then it was possible for overfitting to occur. When the training of the networks was completed, the data for testing which had no effect on the training were applied to the trained models to provide an entire assessment of the network performance independently.

To determine the optimum BPNN, RBFNN and ELM model, the mean square error (MSE) of all the models were monitored during the stages of training and testing. Also, mean absolute error (MAE), Legate and McCabe index (LM), mean absolute percentage error (MAPE) and noise to signal ratio (NSR), were used for judging the performance of the models used. After many trials, the model having the lowest MAPE value was selected as the best model.

III. THEORETICAL CONCEPT OF THE ANN METHODS

This The following presents a brief overview of the backpropagation neural network, radial basis function neural network and extreme learning machine.

3.1 Back Propagation Neural Network (BPNN)

BPNN is the commonest neural network which is mostly applied in many disciplines in which management science and engineering is not an exception. The network simplicity structure design, robust capability, and availability of a large number of training algorithms are some of the utmost reasons. The BPNN is a multilayered network structured into three layers consisting of input layer, hidden layer and the output layer as can be seen in Fig 1. Characteristically, the layers are entirely interconnected. The input layer is the

layer that receives the input information, whereas the output layer gives the final results of the computation. In between the input layer and the output layer is the hidden layer chamber where data transferred from the input layer are analyzed, processed and transferred into the output layer. Literature on BPNN reveals that

only hidden layer is sufficient. Hornik [17] proved that BPNN with one hidden layer is enough to approximate any continuous function. Therefore, one hidden layer was employed in this current study. In this study, the optimum number of neurons in the hidden layer was obtained based on the smallest mean squared error.

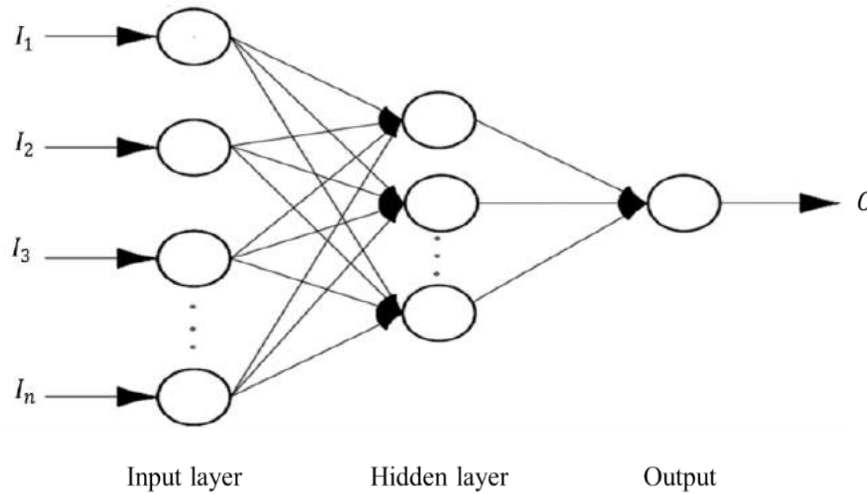


Figure 1: Architecture of the Back Propagation Neural Network with an input layer (I), a hidden layer(h) and an output layer(O).

In addition to the above, the hyperbolic tangent activation function used in the hidden layer was employed to introduce a non-linearity into the network. Selection of hyperbolic tangent activation function which produces output in scale of $[-1,1]$. The hyperbolic tangent activation function used in this study is given in Eq.3 as:

$$f(x) = \tanh(x) = \frac{(e^x - e^{-x})}{(e^x + e^{-x})} \quad (3)$$

Where x is the sum of the weighted inputs. One of the essential aspects to note about back propagation neural network training is that, it can be characterized as a non-linear optimization problem, w^* [18] as indicated in Eq. (4) as:

$$w^* = \arg \min E(w) \quad (4)$$

where w is the weight matrix and $E(w)$ is the error function. To find the optimum weight

connection w^* that minimizes $E(w)$ is the purpose of training the network.

Eq. (2) evaluated at any point of w is given in Eq. (5), Eq. (6), Eq. (7) respectively

$$E(w) = \sum_n E_n(w) \quad (5)$$

where n is the number of training examples and $E_n(w)$ is the output error for each example n .

$E_n(w)$ [18] is mathematically defined by Eq. (6)

$$E(w) = \frac{1}{2} \sum_j (d_{nj} - y_{nj}(w))^2 \quad (6)$$

where d_{nj} and $y_{nj}(w)$ are desired network outputs and estimated values of the j^{th} output neuron for the n^{th} example, respectively. Therefore, substituting Eq. (6) into Eq. (5) gives

the objective function to be minimized expressed in Eq. (7) [18] as:

$$E(w) = \frac{1}{2} \sum_n \sum_j (d_{nj} - y_{nj}(w))^2 \quad (7)$$

In order to arrive at an acceptable value by the error function, the training process continues by adjusting the weights of the output neurons then proceeds towards the input data. There are several numerical optimization algorithms to perform this weight adaptation [19]. In this study, Levenberg-Marquardt algorithm (LMA) was chosen to train the BPNN because it is faster and has more stable convergence compared to the popular gradient descent algorithm proven in the works of Hagan [20]. The LMA is a gradient descent algorithm. The behavior of the algorithm is like steepest descent method when the current solution is far from the correct one, thus the

algorithm approaches the correct solution. Detailed mathematical theory of LMA can be found in [19 and 21].

3.2 Radial Basis Function Neural Network

The RBFNN is a type of ANN which has a feed-forward structure consisting of three layers; the input, hidden and output layers which is indicated in Fig 2. The nodes within each layer are fully connected to the previous layer. Here, the input variables are each assigned to a node in the input layer and transferred to the hidden layer which are unweighted. It can be realized that, the difference between BPNN and RBFNN are that in the RBFNN the connections between the input and hidden layers are unweighted and the activation functions on the hidden layer node are radially symmetric.

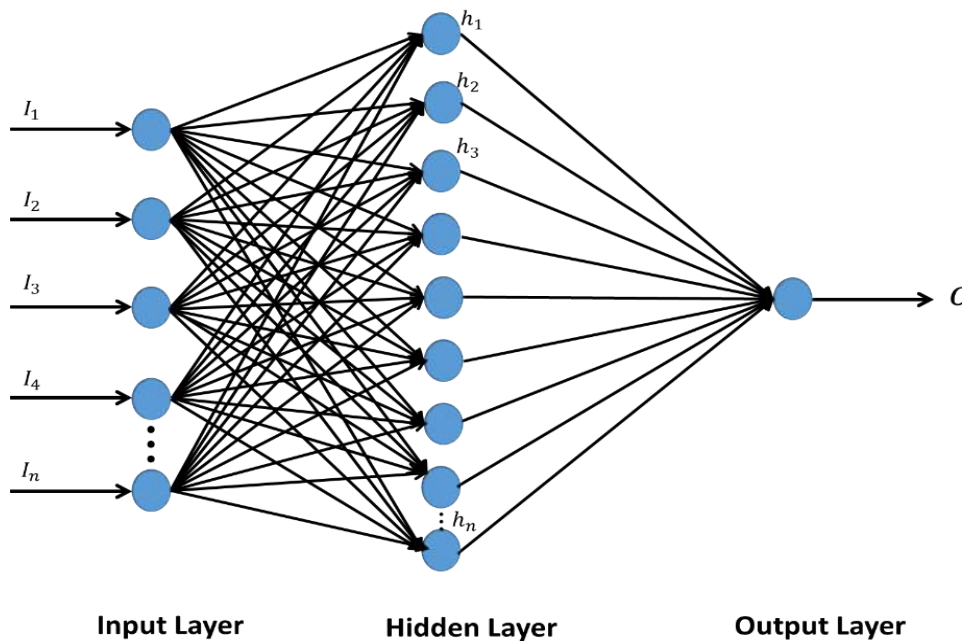


Figure 2: Architecture of the RBF Neural Network Based Load Forecasting Technique.

Within the hidden layer, each neuron calculates a Euclidean norm that shows the distance between the inputs. This is then inserted into a radial basis activation function which calculates and outputs the activation of the neuron. In this present study, the Gaussian activation function was employed and it is expressed in Eq. (8) as:

$$\theta_j(x) = \left[-\frac{\|X - \mu_i\|^2}{2\sigma_j^2} \right] \quad (8)$$

Where, X is the input vector, μ_i is the center of the Gaussian function and σ_j is the spread

parameter of the Gaussian bells and $\| \cdot \|$ is the Euclidean norm. The linear function is contained in the output layer thereby using the weighted sum of the hidden layer as propagation function. Let $o(H)$ be the output of the k th radial basis function on the i th sample. The output of each target node j is computed using the weights w_{jk} indicated in Eq. (9) as:

$$O_{ji} = \sum_n w_{jk} O_{ni}^{(H)} \quad (9)$$

Here, the target output for sample i on target node j be O_{ji} . The error function $E(w)$ [22] is expressed in Eq. (10) as:

$$E(w) = \frac{1}{2} \sum_{ji} \left(\sum_k w_{jk} y_{ki}^{(H)} - Y_{ji} \right)^2 \quad (10)$$

which has its minimum where the derivative Eq.

$$\frac{dE}{dw_{rs}} = \sum_k \sum_i w_{rk} y_{ki}^{(H)} y_{ji}^{(H)} - \sum_i Y_{ri} y_{si}^{(H)} \quad (11)$$

vanishes. Let R be the correlation matrix of the radial basis function outputs given by Eq. (12) as follows

$$R_{jk} = \sum_i y_{ki}^{(H)} y_{ji}^{(H)} \quad (12)$$

The weight matrix w^* Eq. 13 which minimizes E lies where the gradient vanishes

$$w_{jk}^* = \sum_r \sum_i Y_{ri} y_{ri}^{(H)} (R^{-1})_{rk} \quad (13)$$

Thus, the problem that is solved when the square $H \times H$ Matrix R is inverted, where H represents the number of radial basis function. The singular value decomposition (SVD) approach can be used to solve the matrix inversion whereas diagonalising the matrix provides an approximate inverse. A parameter inverts the eigenvalues

which exceeds zero- specified margin and transformed back to the original coordinates, providing an optimal minimum-norm approximation to the inverse in the least-mean-squares sense [22]. This training process continues until the network error reaches an acceptable value.

3.3 Extreme Learning Machine

The ELM model constitutes an input layer, a single-hidden layer, and an output layer. All parameters including the input, weights and hidden bias are determined by iterative network in solving a particular problem [23-24]. As illustrated in Fig 3, the main idea in ELM is that the network hidden layer parameters need not to be learned, but can be randomly assigned. The network output weights can be subsequently and analytically calculated while the input weights are randomly chosen. For hidden neurons, there are several activation functions such as sigmoidal, sine, Gaussian and hard-limiting function that can be used, and the output neurons have linear activation function.

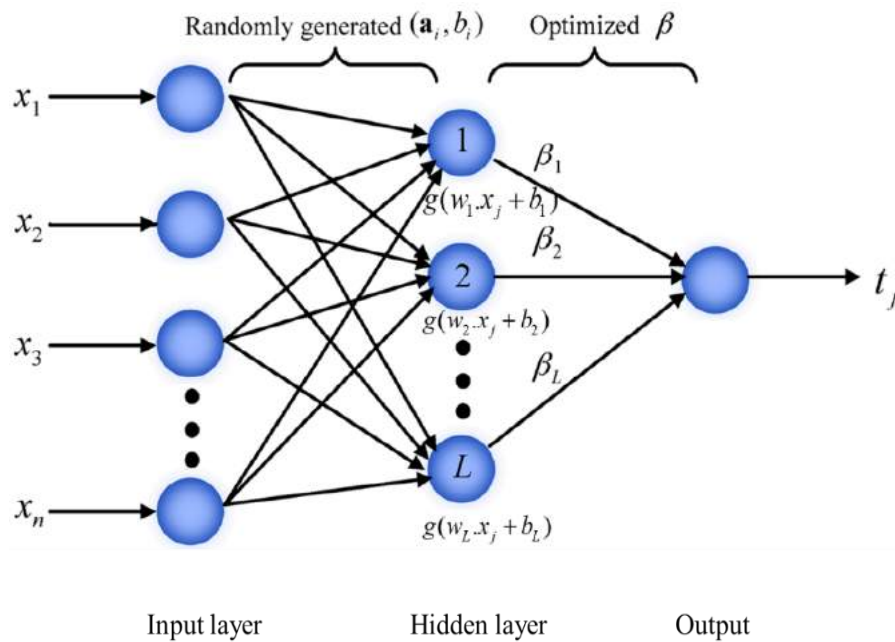


Figure 3: Architectural Design of an ELM Predictor.

Briefly, the basic theory of the ELM model states that for N arbitrary distinct input samples $(x_k, y_k) \in \mathbb{R}^n \times \mathbb{R}^n$, the standard SLFNs with M hidden nodes and an activation function is mathematically described in Eq. (14) as:

$$\sum_{i=1}^M \beta_i g(x_k; c_i, a_i) = y_k \quad k = 1, 2, 3, \dots, N \quad (14)$$

where $c_i \in \mathbb{R}$ is the randomly assigned bias of the i th hidden node and $w_i \in \mathbb{R}$ is the randomly assigned input weight vector connecting the i th hidden node and the input nodes. β_i is the weight vector connection the i th hidden node to the output node. $g(x_k; c_i, w_i)$ is the output of the i th hidden node with respect to the input sample x_k . Each input is randomly assigned to the hidden nodes in ELM network. Then, Eq. (14) can be simplified in Eq. (15) as:

$$H\beta = Y \quad (15)$$

IV. ANN APPLICATION

4.1 Development of ANN Models

The development of a suitable ANN model to accurately predict the monthly load consumption

demand in different sectors is the main aim for this current research. Five sectors: the residential sector, the commercial sector, the industrial sector, the transportation sector and the electric power sector with one balancing item have been taken into consideration. The input and output observed dataset was collected from the U.S. Energy Administration for a period of 44 years from January 1973 through May 2017 and divided into two sub-datasets (training and testing datasets) in a random manner. Yet, extreme measures were taken to prevent repetition of the data in any way.

Three ANN models (BPNN, RBFNN and ELM) for the monthly load consumption prediction were developed after which the performance of the ANN predictions were measured by comparing the prediction outputs with the observed output. The proposed ANN models comprised of three layers being the input layer, the hidden layer and the output layer. Each layer is made up of processing element called neurons. The final output is calculated from the processed neurons in the input and hidden layer.

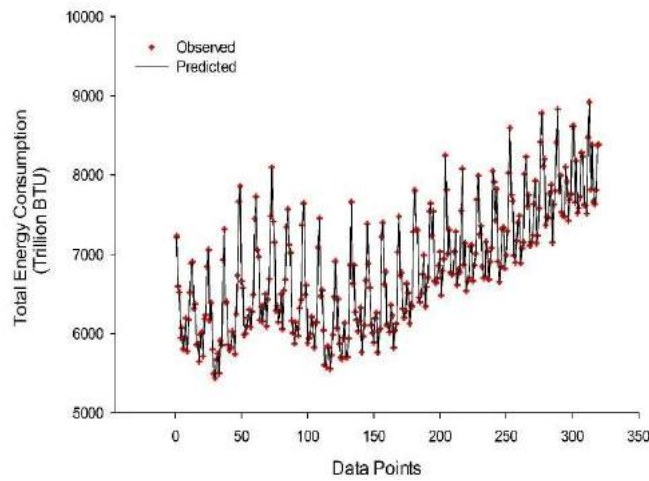


Figure 4a: Training data prediction results for backpropagation neural network (BPNN)

To develop the BPNN, RBFNN and ELM models, the dataset for this research was divided into training and testing sets, as explained in section 3. The supervised learning procedure was applied to the three models (BPNN, RBFNN and ELM). With supervised learning, inputs and observed outputs are provided in the models where residential sector, commercial sector, industrial sector, transportation sector, electric power sector as well as the balancing item serves as the input whiles primary energy consumption total serves as the

observed output respectively. The data was normalized between $[-1$ and $1]$ using a hyperbolic tangent function from the input layer to a single hidden layer for both BPNN. RBFNN model was normalized using the Gaussian function which mimic the non-linearity activation function and an output layer consisting of a linear activation function. Also the ELM model was normalized between $[0,1]$ using the Sigmoid activation function.

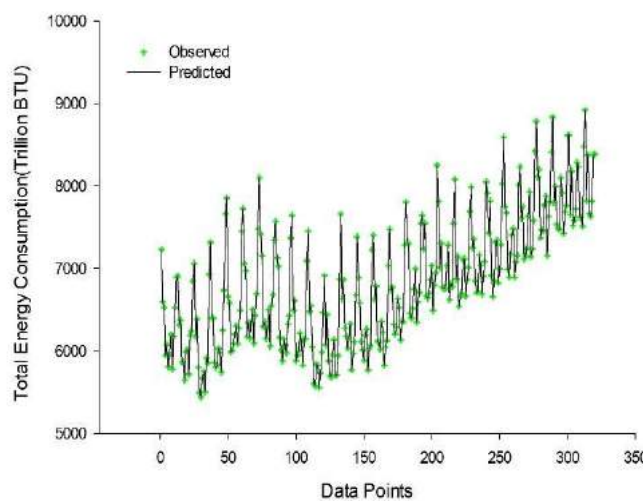


Figure 4b: Training data prediction results for radial basis function neural network (RBFNN)

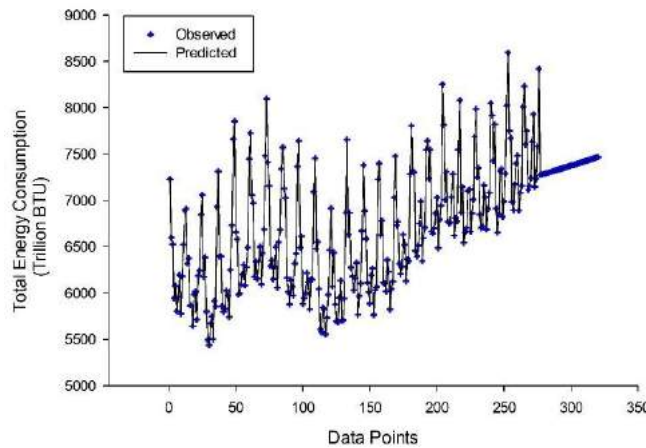


Figure 4c: Training data prediction results for extreme learning machine (ELM)

Moreover, after the network was trained for 1000 epochs, using the Levenberg- Marquardt backpropagation algorithm with a learning rate of 0.03 and a momentum coefficient of 0.7 for the BPNN model, the structure constituted of [6-8-1] that is six inputs, one single hidden layer and one output layer. Also, with the RBFNN model, gradient decent learning algorithm was used to train the network through which the weight is adopted in part to the deviation between the observed and the predicted output. The optimum RBFNN structure was [6-40-1, 39] indicating six inputs, forty hidden neurons and one output in addition to 39 spreads. Finally, the ELM model was training using the sigmoid activation function. The optimum ELM structure was [6-461-1] indicating six inputs, four hundred and sixty-one hidden neurons and one output. Fig. 4a indicates the training data prediction results for backpropagation neural network (BPNN) Fig. 4b shows the radial basis function neural network (RBFNN) training data prediction results whiles Fig 4c shows the training data prediction results of the extreme learning machine (ELM). Likewise, the testing data prediction results for backpropagation neural network (BPNN) radial basis function neural network Additionally, for both the training and testing data sets, the structures for BPNN, RBFNN, and ELM models that yielded the best results were chosen as a result of the least mean square error (MSE), the mean absolute error (MAE) and noise to signal ratio (NSR).

4.2. Assessment of Model Performance and Error Statistics

An evaluation was done on the BPNN, RBFNN and ELM models' performance and error statistics for both training and testing data. This was done by observing the differences between the observed training and testing data that were predicted by BPNN, RBFNN and the ELM models. The performance indicators used in this research were the mean square error (MSE), relative percentage error (RPE) and noise to signal ratio (NSR). In the works of Solmaz & Ozgoren (2012), the mean square error (MSE) and the mean absolute error (MAE) are defined in Eqs. (16) and Eq. (17) and noise to signal ratio (NSR) was added in Eq. (18) as:

$$MSE = \frac{\sum_{i=1}^N e_i^2}{N} \quad (16)$$

$$MAE = \frac{1}{N} \sum_{i=1}^N |O_i - P_i| \quad (17)$$

$$NSR = \frac{\sqrt{\left[\frac{1}{N-1} \sum_{i=1}^N (O_i - P_i)^2 \right]}}{\sigma} \quad (18)$$

where O_i is the observed monthly load consumption, P_i is the predicted monthly load consumption and N is the total number of data.

The mean square error (MSE) indicates the level of scatter that the ANN model produces. The mean absolute error (MAE) is defined as a quantity used to measure how close the predicted values are to the observed values. And the noise to signal ratio compares the level of the desired signal to the level of background noise. In other to have a good prediction accuracy of the ANN model, a lower MSE is needed. Nevertheless, the ANN model with lower values of MSE, MAE and NSR is used to evaluate the best model for prediction.

Tables 1 and 2 indicate the BPNN, RBFNN and ELM models' performance in terms of the mean square error (MSE), mean absolute error (MAE) and noise to signal ratio (NSR) for the observed and predicted load consumption. Training and testing datasets were all evaluated using the MSE, MAE and NSR for the various number of neurons. The best model for predicting the monthly load consumption was selected based on Tables 1 and 2. From the analysis of the results, the optimum

model for predicting the monthly load consumption was BPNN in which values obtained in terms of the minimum MAE values were 0.000796433 and 0.008201697 for training and testing results respectively. The minimum value for MSE for BPNN which gave the optimum model for predicting the monthly load consumption were 0.00000143704 and 0.000189 for training and testing results respectively. The minimum value for NSR for BPNN which gave the optimum model for predicting the monthly load consumption were 0.000000175949 and 0.0000016891 for training and testing results respectively. Hence the BPNN proves the best artificial neural network method for predicting the monthly load consumption in this present research. The testing data prediction results for backpropagation neural network, radial basis function neural network as well as extreme learning machine is shown in Fig 5a, 5b and 5c respectively.

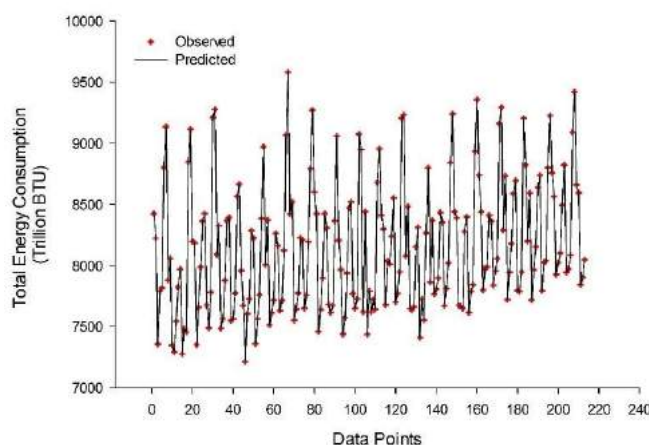


Figure 5a: Testing data prediction results for backpropagation neural network (BPNN)

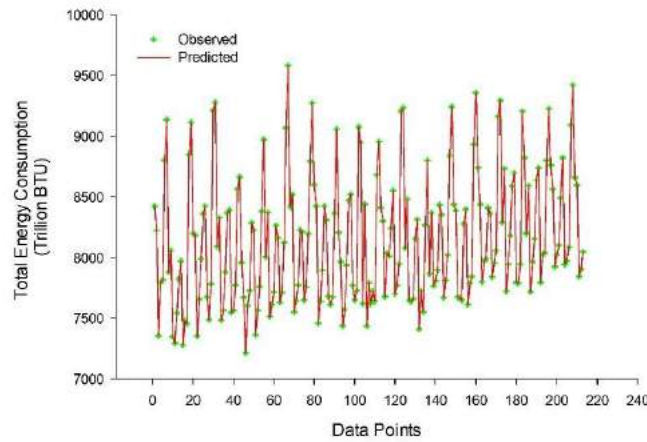


Figure 5b: Testing data prediction results for radial basis function neural network (RBFNN)

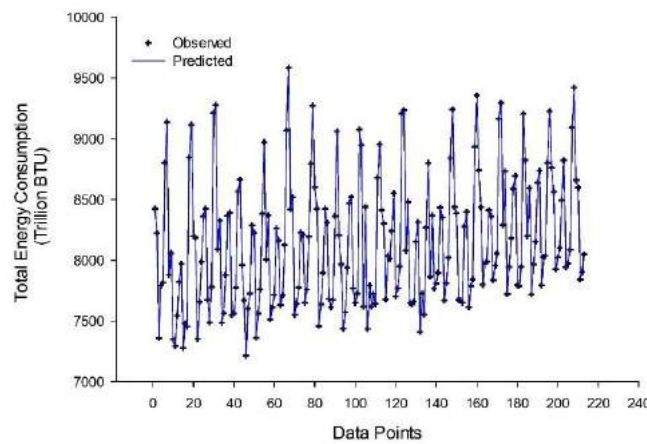


Figure 5c: Testing data prediction results for extreme learning machine (ELM)

4.3. Statistics-Based Dimension for Model Efficiency

Likewise, in Table (1-4), three other model efficiency based statistics, relative percentage error (REL), Legates and McCabe index (LM), mean absolute percentage error (MAPE) were also employed to access the model efficiency are expressed in Eqs. (19) to (21) respectively as:

$$REL = 1 - \sum_{i=1}^N \frac{|e_i|}{O_i} \quad (19)$$

$$LM = 1 - \frac{\sum_{i=1}^N ABS(O_i - P_i)}{\sum_{i=1}^N ABS(O_i - \sigma)} \quad (20)$$

$$MAPE = \frac{\sum_{i=1}^N \left| \frac{O_i - P_i}{O_i} \right|}{N} \quad (21)$$

where $e_i = O_i - P_i$, O_i is the observed output load consumption, P_i is the predicted output load consumption and i is an integer that varies from 1.

Table 1: Model Efficiency-Based Statistic Indicators for the Monthly load forecasting for Training

MODEL	BPNN	RBFNN	ELM
MSE	0.00000143704	0.001136	0.001343
MAE	0.000796433	0.025858341	0.028353654
NSR	0.000000175949	0.00000494784	0.00000537913

Table 2: Model Efficiency-Based Statistic indicators for the Monthly load forecasting for Testing

MODEL	BPNN	RBFNN	ELM
MSE	0.000189	0.012137	0.824947
MAE	0.008201697	0.102506253	0.729468184
NSR	0.0000016891	0.0000135449	0.000111668

Table 3: Statistical indicators for the Monthly load forecasting (Training Performance)

MODEL	BPNN	RBFNN	ELM
LM	0.999999905	0.999999975	0.000000389
REL	0.999963075	0.998763497	0.998642
MAPE	0.999999885	0.999996136	0.999996

Table 4: Statistical indicators for the Monthly load forecasting (Testing Performance)

MODEL	BPNN	RBFNN	ELM
LM	0.999996092	0.000008314	0.000112
REL	0.999801642	0.997317	0.981328
MAPE	0.999999069	0.999987406	0.999912336

From the analysis of the result shown in Tables 3 and 4, the optimum model for predicting the monthly load consumption was BPNN in which values obtained in terms of the LM values were 0.999999905 and 0.999996092 for training and testing results respectively. The value for REL for BPNN which gave the optimum model for predicting the monthly load consumption were 0.999963075 and 0.999801642 for training and testing results respectively. The value for MAPE for BPNN which gave the optimum model for predicting the monthly load consumption were 0.999999885 and 0.999999069 for training and testing results respectively. Prediction error results training data, testing data for backpropagation neural network (BPNN), radial basis function neural network (RBFNN) and extreme learning machine (ELM) has been shown in Fig. 6a and 6b above.

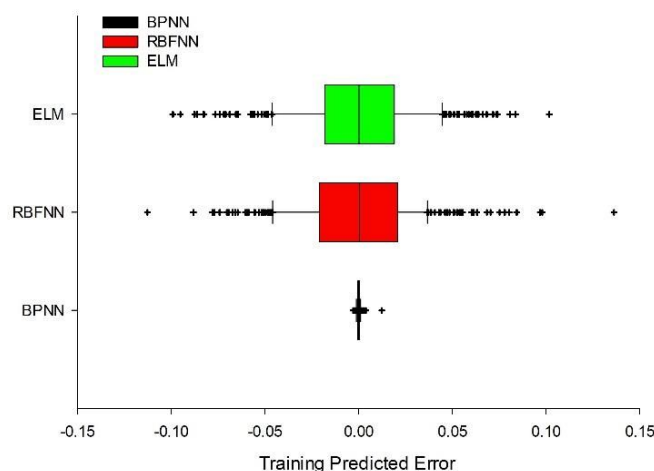


Figure 6a: Prediction error results for training data for backpropagation neural network (BPNN), radial basis function neural network (RBFNN) and extreme learning machine (ELM)

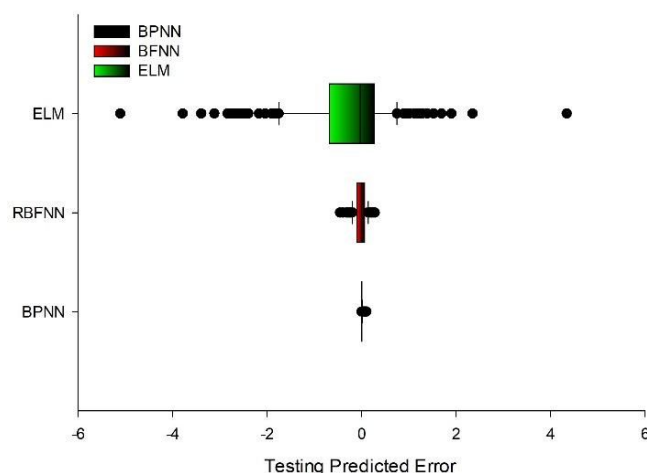


Figure 6b: Prediction error results for testing data for backpropagation neural network (BPNN), radial basis function neural network (RBFNN) and extreme learning machine (ELM)

V. CONCLUSION

A vital role when considering electrical energy systems, energy supply, planning and operation is an accurate short-term load forecast. This research is aimed to develop an ANN model for accurate prediction of monthly load consumption demand. Therefore, this research has presented the Back Propagation neural network (BPNN), Radial Basis function neural Network (RBFNN) based on supervised learning technique and Extreme Learning Machine (ELM) as a forecasting model to predict a monthly load consumption demand. The dataset was grouped into training and testing data sets. The minimum mean absolute error and MAPE was used as a performance indicator in choosing the optimum

models for the load forecasting. Findings from this researched revealed that, the BPNN, RBFNN and ELM offered a satisfactory prediction of the short term monthly load forecasting. Assessment of the models were made by correlating predicted values and observed values where values close to +1 signified a good fit. Also, the mean square errors for both training and testing processes were obtained where errors close to 0 indicated a good prediction. From the analysis of the results, it was found that the predicted values are in good agreement with measured values as the best artificial neural network for predicting the monthly load forecasting is the BPNN comparatively with lower Mean Square Error (MSE) as compared to the RBFNN and the ELM.

This can therefore be concluded that, BPNN is a vital tool to achieve optimum results for short term monthly load forecasting.

REFERENCES

1. Bhattacharyya, S. C. and Timilsina, G. R. (2009) 'Energy Demand Models for Policy Formulation a Comparative Study of Energy Demand Models', *Energy*, 4866(March), p. 151. doi: 10.1596/1813-9450-4866.
2. Shah, M. and Agrawal, R. (2013) 'A Review On Classical and Modern Techniques with Decision Making Tools for Load Forecasting', 6(3), pp. 174–184.
3. Tsekouras, G. J., Kanellos, F. D. and Mastorakis, N. (2015) Short Term Load Forecasting in Electric Power Systems with Artificial Neural Networks. doi: 10.1007/978-3-319-15765-8.
4. Azadeh, A., Seraj, O. and Saberi, M. (2011) 'An integrated fuzzy regression-analysis of variance algorithm for improvement of electricity consumption estimation in uncertain environments', *International Journal of Advanced Manufacturing Technology*, 53(5–8), pp. 645–660. doi: 10.1007/s00170-010-2862-5.
5. Guo, J. J., Wu, J. Y. and Wang, R. Z. (2011) 'A new approach to energy consumption prediction of domestic heat pump water heater based on grey system theory', *Energy and Buildings*, 43(6), pp. 1273–1279. doi: 10.1016/j.enbuild.2011.01.001.
6. Mandal, P. et al. (2006) 'A neural network based several-hour-ahead electric load forecasting using similar days' approach', *International Journal of Electrical Power and Energy Systems*, 28(6), pp. 367–373. doi: 10.1016/j.ijepes.2005.12.007.
7. Kandil, N. et al. (2006) 'An efficient approach for short term load forecasting using artificial neural networks', *International Journal of Electrical Power & Energy Systems*, 28(8), pp. 525–530. doi: 10.1016/j.ijepes.2006.02.014.
8. Yao, R. and Steemers, K. (2005) 'A method of formulating energy load profile for domestic buildings in the UK', *Energy and Buildings*, 37(6), pp. 663–671. doi: 10.1016/j.enbuild.2004.09.007
9. Tang, Z. and Fishwick, P. a. (1993) 'Feedforward Neural Nets as Models for Time Series Forecasting', *INFORMS Journal on Computing*, 5(4), pp. 374–385. doi: 10.1287/ijoc.5.4.374.
10. US Energy Information Administration (2016) How much electricity is used for lighting in the United States? - FAQ - U.S. Energy Information Administration (EIA), www.eia.gov. Available at: <https://www.eia.gov/tools/faqs/faq.cfm?id=99&t=3>.
11. Kohzadi, N. et al. (1996) 'A comparison of artificial neural network and time series models for forecasting commodity prices', *Neurocomputing*, 10(2), pp. 169–181. doi: 10.1016/0925-2312(95)00020-8.
12. Hagan, M. T. and Menhaj, M. B. (1994) 'Training Feedforward Networks with the Marquardt Algorithm', *IEEE Transactions on Neural Networks*, 5(6), pp. 989–993. doi: 10.1109/72.329697.
13. Azadeh, A., Ghaderi, S. F. and Sohrabkhani, S. (2007) 'Forecasting electrical consumption by integration of Neural Network, time series and ANOVA', *Applied Mathematics and Computation*, 186(2), pp. 1753–1761. doi: 10.1016/j.amc.2006.08.094.
14. Worrell, E., Ramesohl, S. and Boyd, G. (2004) 'Advances In Energy Forecasting Models Based On Engineering Economics', *Annual Review of Environment and Resources*, 29(1), pp. 345–381. Doi:10.1146/annurev.energy.29.062403.102042.
15. Karl, T. R. et al. (2010) 'Observation needs for climate information, prediction and application: Capabilities of existing and future observing systems', in *Procedia Environmental Sciences*, pp. 192–205. doi: 10.1016/j.proenv.2010.09.013.
16. Larochelle, H. et al. (2009) 'Exploring Strategies for Training Deep Neural Networks', *Journal of Machine Learning Research*, 1, pp. 1–40. doi: Doi 10.1109/Tsmcc.2012.2220963.

17. Hornik, K., Stinchcombe, M. and White, H. (1989) 'Multilayer feedforward networks are universal approximators', *Neural Networks*, 2(5), pp. 359–366. doi: 10.1016/0893-6080(89)90020-8.
18. Konaté, A. A. et al. (2014) 'Prediction of porosity in crystalline rocks using artificial neural networks: An example from the Chinese Continental Scientific Drilling Main hole', *Studia Geophysica et Geodaetica*, 59(1), pp. 113–136. doi: 10.1007/s11200-013-0993-5.
19. Milanič, M. et al. (2011) Numerical optimization of sequential cryogen spray cooling and laser irradiation for improved therapy of port wine stain, *Lasers in Surgery and Medicine*. doi: 10.1002/lsm.21040.
20. Hagan, M. T. and Menhaj, M. B. (1994) 'Training Feedforward Networks with the Marquardt Algorithm', *IEEE Transactions on Neural Networks*, 5(6), pp. 989–993. doi: 10.1109/72.329697.
21. Lourakis, M. I. a (2005) 'A Brief Description of the Levenberg-Marquardt Algorithm Implemented by levmar', *Matrix*, 3, p. 2. doi: 10.1016/j.ijinfomgt.2009.10.001.
22. Michie D, Spiegelhalter DJ, Taylor CC (1994) *Machine learning, neural and statistical classification*. Ellis Horwood, Upper Saddle River, NJ, USA.
23. Parikh, P. J. and Lam, S. S. (2009) 'Solving the forward kinematics problem in parallel manipulators using an iterative artificial neural network strategy', *International Journal of Advanced Manufacturing Technology*, 40(5–6), pp. 595–606. doi: 10.1007/s00170-007-1360-x.
24. Huang, G., Zhu, Q. and Siew, C. (2004) 'Extreme Learning Machine: A New Learning Scheme of Feedforward Neural Networks', *IEEE International Joint Conference on Neural Networks*, 2, pp. 985–990. doi: 10.1109/IJCNN.2004.1380068.

This page is intentionally left blank



Scan to know paper details and author's profile

Some Features of a Gravitational Field Quantization

A.N. Volobuev

Samara State Medical University

ABSTRACT

The problems connected to propagation of a gravitational field are considered. The law of change of an electromagnetic radiation frequency in a gravitational field is shown. On the basis use of a quantum gravitational eikonal the energy of a single graviton is found. Refusal from a stresses tensor in structure of an energy-impulse tensor has allowed the quantum form of the energy-impulse tensor in Einstein's equation is found. It is shown that the solution of the Einstein's equation for the certain direction in this case represents the sum of a gravitational wave and a graviton. It is noticed that the deep understanding of process of the gravitational waves with massive body interaction can be only at the quantum philosophy. It is shown that at approach of a graviton to the massive bodies (double stars) radiating gravitational waves there is a resonant pumping of the gravitational field energy of these bodies to the gravitons. It enables registration of the gravitons with the help of the detector located near to massive bodies.

Keywords: a gravitational eikonal, metric tensor, einstein's equation, energy flux, gravitational waves, energy-impulse tensor, registration of gravitons.

Classification: FOR code: 020105

Language: English



London
Journals Press

LJP Copyright ID: 925642
Print ISSN: 2631-8490
Online ISSN: 2631-8504

London Journal of Research in Science: Natural and Formal

Volume 19 | Issue 2 | Compilation 1.0



Some Features of a Gravitational Field Quantization

A.N. Volobuev

ABSTRACT

The problems connected to propagation of a gravitational field are considered. The law of change of an electromagnetic radiation frequency in a gravitational field is shown. On the basis use of a quantum gravitational eikonal the energy of a single graviton is found. Refusal from a stresses tensor in structure of an energy-impulse tensor has allowed the quantum form of the energy-impulse tensor in Einstein's equation is found. It is shown that the solution of the Einstein's equation for the certain direction in this case represents the sum of a gravitational wave and a graviton. It is noticed that the deep understanding of process of the gravitational waves with massive body interaction can be only at the quantum philosophy. It is shown that at approach of a graviton to the massive bodies (double stars) radiating gravitational waves there is a resonant pumping of the gravitational field energy of these bodies to the gravitons. It enables registration of the gravitons with the help of the detector located near to massive bodies.

Keywords: a gravitational eikonal, metric tensor, Einstein's equation, energy flux, gravitational waves, energy-impulse tensor, registration of gravitons.

Author: Samara State Medical University, Department of Physics.

I. INTRODUCTION

The modern theory of gravitation - the theory general relativity of Einstein - is a basis for calculation of the various phenomena. It is generalization Newtonian dynamics, including the law of universal gravitation. As well as Newtonian

dynamics the theory general relativity is not the quantum theory. The Einstein's equation for a gravitational field does not have stochastic nature.

Obviously such situation is unacceptable however the problem of a gravitational field quantization till now is not solved though for the solving of this problem many efforts have been applied [1-4].

Recently the problem of gravitational waves detecting [5] which description is possible with the help of the Einstein's equation [6] of general relativity is solved. This is one more experimental confirmation of validity of the theory general relativity.

From the physical point of view the general relativity theory assumes that the mass curvatures a space-time. This curvature of space-time influences all particles moving in space, including and what create a curvature. Influence is carried out and on massless particles, for example - photons. It is connected to a curvature of geodetic lines of space-time on which photons move. Photons change the frequency in a gravitational field. Space-time curvature in the general relativity theory identify with occurrence of some gravitational field due to which there is an interaction of mass particles.

Gravitational waves are propagating oscillations of the curved space-time as similar the waves on a water surface are propagating oscillations of the water particles.

However in the submitted physical picture of gravitation there is no the major element-quantization of a gravitational field.

Attempts to solve a problem of the gravitational waves quantization with the help of 5-dimensional space-time use [7] can hardly lead to success.

Apparently, the theory of 5-dimensional space-time now has only a historical value. By comparison of distance from the source of gravitational waves calculated by the attenuation of experimentally registered gravitational waves and by the red displacement of electromagnetic radiation it has been established [8] that dimension of our space-time is equal $\sim 4 \pm 0,1$. Thus our space-time is described by four coordinates: time and three spatial coordinates.

The quanta of a gravitational field refer to gravitons. Gravitons represent a local wrinkling of the space-time which is propagated on more smooth space with a light velocity. Assuming as a whole correctness of the Einstein's equation for a gravitational field we research some features of the gravitational waves quantization.

II. PHOTON IN CONSTANT HOMOGENEOUS GRAVITATIONAL FIELD

For the beginning to a gravitational field quantization we shall consider how frequency of an electromagnetic radiation quantum (photon) in a constant homogeneous gravitational field changes. Research we shall carry out in flat space-time the name Minkowski's space. The interval in inertial reference system looks like [6]:

$$ds^2 = c^2 d\tau^2 - dX^2 - dY^2 - dZ^2 = g_{00}(dX^0)^2 - g_{11}(dX^1)^2 - g_{22}(dX^2)^2 - g_{33}(dX^3)^2, \quad (1)$$

where designations there are $X = X^1, Y = X^2, Z = X^3$ - the Cartesian coordinates, c - a light velocity in vacuum, $d\tau$ - an interval proper time between events, so $cd\tau = dX^0$, $g_{00} = 1, g_{11} = g_{22} = g_{33} = -1$ - the metric tensor components which signature $(+, -, -, -)$.

From (1) follows:

$$d\tau = \frac{1}{c} \sqrt{g_{00}} dX^0. \quad (2)$$

In a gravitational field $g_{00} < 1$. Therefore, proper (or own) time flows that more slowly than is less g_{00} in the given point of space ($\Delta\tau = \tau_2 - \tau_1$

decreases; τ_2 in field it is less τ_2 outside of field). The clock per a gravitational field is slow.

The component of metric tensor g_{00} in a gravitational field decreases:

$$g_{00} = \left(1 + \frac{\varphi_g}{c^2}\right)^2 \text{ or } \sqrt{g_{00}} = 1 + \frac{\varphi_g}{c^2}, \quad (3)$$

where is φ_g gravitational potential of a field, negative size so that acceleration $\dot{V} = -\text{grad}\varphi_g$.

For the further analysis we use concept of an eikonal. Eikonal there is a phase of the periodic function describing a field of electromagnetic wave:

$$\phi = \mathbf{k}\mathbf{q} - \delta\tau, \quad (4)$$

where \mathbf{k} there is a wave vector of an eikonal, \mathbf{q} - a coordinate vector of an eikonal (it is optional Cartesian), δ - cyclic frequency of the eikonal.

Taking into account (2) and (4) it is possible to find the eikonal frequency (a photon frequency in the given point in a proper time):

$$\delta = -\frac{\partial\phi}{\partial\tau} = -\frac{\partial\phi}{\partial X^0} \frac{\partial X^0}{\partial\tau} = -\frac{c}{\sqrt{g_{00}}} \frac{\partial\phi}{\partial X^0}. \quad (5)$$

If to use the world time t (outside of a gravitational field), so that $t = \frac{X^0}{c}$ the photon

cyclic frequency measured in world time is equal

$$\delta_0 = -\frac{\partial\phi}{\partial t} = -c \frac{\partial\phi}{\partial X^0}. \text{ Hence, according to (5) with}$$

the account (3) we have:

$$\delta = \frac{\delta_0}{\sqrt{g_{00}}} = \frac{\delta_0}{1 + \frac{\varphi_g}{c^2}}. \quad (6)$$

where δ_0 there is photon frequency at absence of a gravitational field.

Thus photon frequency depends on size of a gravitational field potential. As the gravitational field potential it is negative size at approach to the creating a field bodies, the photon frequency δ grows, and at removal falls (red displacement).

For example, for a body in mass M the potential of a field depends on radius r under the formula

$$\varphi_g = -k \frac{M}{r} \quad \text{where} \quad k = 6.67 \cdot 10^{-8} \frac{cm^3}{g \cdot s}$$

there is gravitational constant.

If the concept of eikonal to a gravitational field apply the formula (6) should be correct and for gravitational waves.

The eikonal wave vector (or a photon wave vector)

$$\mathbf{k} = \frac{\partial \phi}{\partial \mathbf{q}}, \quad \text{and 4-impulse in the Cartesian}$$

coordinates is equal $k_i = -\frac{\partial \phi}{\partial X_i}$. But for the 4-

impulse the formula $k_i k^i = k^0 k^0 - \mathbf{k}\mathbf{k} = 0$ is

correct. Hence, $\frac{\partial \phi}{\partial X_i} \frac{\partial \phi}{\partial X^i} = 0$ there is the eikonal

equation.

Let's note that the eikonal is a quantized size. The eikonal quantum is equal:

$$S_0 = \hbar \phi, \quad (7)$$

where \hbar there is reduced Planck's constant.

III. THE EINSTEIN'S EQUATION FOR A GRAVITATIONAL FIELD

The gravitational field is described by the Einstein's equation. For writing of the Einstein's equation it is necessary first of all by the mathematical to describe a curvature of space-time. For the description of the mathematical curvature of space-time it is used a tensor of curvature (Riemann's tensor) [6]:

$$R_{iklm} = \left(\frac{\partial \Gamma_{km}^i}{\partial X^l} - \frac{\partial \Gamma_{kl}^i}{\partial X^m} \right) + \left(\Gamma_{nl}^i \Gamma_{km}^n - \Gamma_{nm}^i \Gamma_{kl}^n \right), \quad (8)$$

Where Γ_{kl}^i there is a projection of a derivative unit vector \mathbf{e}_k on coordinate X^l on a coordinate

axis X^i - Cristoffel's symbol $\Gamma_{kl}^i \mathbf{e}_i = \frac{\partial \mathbf{e}_k}{\partial X^l}$.

Cristoffel's symbols it is the functions of coordinates characterizing change a component of a vector at its parallel displacement. All indexes, bottom (covariant, usually functional sizes) and

top (contravariant, usually coordinate sizes) accept values 0 (a time index), 1, 2, 3 (coordinate indexes). As it is usual summation is carried out on indexes repeating in products.

Cristoffel's symbols can be expressed through metric tensor under the formula

$$\Gamma_{kl}^i = \frac{1}{2} g^{im} \left(\frac{\partial g_{mk}}{\partial X^l} + \frac{\partial g_{ml}}{\partial X^k} - \frac{\partial g_{kl}}{\partial X^m} \right) \quad [6]. \quad \text{Thus}$$

curvature tensor of a space-time it is determined by a velocity and rapidly of a metric tensor g_{ik}

change in the space - time. Generally there are 10 components of a metric tensor: 4 - with identical indexes (00, 11, 22, 33), and 6 with different

indexes (01, 02, 03, 12, 13, 23, $C_4^2 = \frac{4 \cdot 3}{1 \cdot 2} = 6$).

The curvature tensor is a fourth rank. Physically the curvature of space-time can be described only the second rank tensor since energy-impulse tensor creating this curvature is the second rank tensor. Therefore we shall pass with the help of a curtailing operation in (7) to the second rank tensor (Ricci's tensor):

$$R_{ik} = g^{lm} R_{limk} = \left(\frac{\partial \Gamma_{ik}^l}{\partial X^l} - \frac{\partial \Gamma_{il}^l}{\partial X^k} \right) + \left(\Gamma_{ik}^l \Gamma_{lm}^m - \Gamma_{il}^m \Gamma_{km}^l \right). \quad (9)$$

The Ricci's tensor it is symmetrical $R_{ik} = R_{ki}$.

Further we shall introduce a scalar curvature of a space-time under the formula:

$$R = g^{ik} R_{ik}, \quad (10)$$

where g^{ik} there is contravariant metric tensor.

Using the Ricci's tensor (9), a scalar curvature of a space-time (10), and also a metric tensor g_{ik} , the Einstein has written down the basic equation for a gravitational field:

$$R_{ik} - \frac{1}{2} g_{ik} R = \frac{8\pi k}{c^4} T_{ik}. \quad (11)$$

The left part of this equation refers to Einstein's tensor $E_{ik} = R_{ik} - \frac{1}{2} g_{ik} R$. It characterizes

geometrical properties of a space-time in particular its curvature. The right part of the equation includes an energy-impulse tensor of the

second rank describing the source which creates the curvature of a space-time:

$$T_{ik} = \begin{pmatrix} T_{00} & T_{01} & T_{02} & T_{03} \\ T_{10} & T_{11} & T_{12} & T_{13} \\ T_{20} & T_{21} & T_{22} & T_{23} \\ T_{30} & T_{31} & T_{32} & T_{33} \end{pmatrix} \quad (12)$$

Einstein's equation (11) can be written down in the other kind. We shall multiply at left the equation (11) on the contravariant metric tensor g^{ik} :

$$g^{ik} R_{ik} - \frac{1}{2} g^{ik} g_{ik} R = \frac{8\pi k}{c^4} g^{ik} T_{ik}. \quad (13)$$

Taking into account $R = g^{ik} R_{ik}$ and $g^{ik} g_{ik} = 4$ (in a four-dimensional space-time) we shall find:

$$-R = \frac{8\pi k}{c^4} \text{Sp} T_{ik} = \frac{8\pi k}{c^4} T, \quad (14)$$

where it is designated $\text{Sp} T_{ik} = T$.

$$s = \int l \sqrt{-g} dt = \int (T - U) \sqrt{-g} dt = \int T \sqrt{-g} dt - \int U \sqrt{-g} dt, \quad (16)$$

where $l = T - U$ there is total Lagrangian of a system a gravitational field - particle and their interaction [9], $\sqrt{-g}$ - defines the dependence of an volume normalizing element on space-time curvature, g - the determinant of a metric tensor. Let's consider Lagrangian l of a systems a gravitational field - particle. It looks like:

$$l = T - U = (\rho - \rho_0) c^2 - (\rho \varphi_g - l_g), \quad (17)$$

where $T = (\rho - \rho_0) c^2$ there is the volumetric density of a kinetic energy of a particle in a gravitational field, $U = (\rho \varphi_g - l_g)$ - volumetric density of a potential energy of a particle in a field (energy of interaction of a particle and field) including Lagrangian of the field [6]:

$$l_g = \frac{c^4}{16\pi k} R, \quad (18)$$

$$w = \dot{q} \frac{\partial l}{\partial \dot{q}} - l = \sqrt{2T} \frac{\partial l}{\partial \sqrt{2T}} - T + U = \sqrt{T} \frac{\partial l}{\partial T} \frac{\partial T}{\partial \sqrt{T}} - T + U = T + U, \quad (21)$$

Having substituted (14) in the Einstein's equation (11) we shall find:

$$R_{ik} = \frac{8\pi k}{c^4} \left(T_{ik} - \frac{1}{2} g_{ik} T \right). \quad (15)$$

Outside of a spherical symmetric body in mass M creating a gravitational field the energy-impulse tensor is equal to zero $T_{ik} = T = 0$. In this case according to (15) $R_{ik} = 0$.

Zero size of the Ricci's tensor according to the equation does not mean that there is no curvature of a space-time. The space-time curvature which is characterized by the Riemann's tensor (7) is kept in distance from the bodies creating this curvature.

IV. Action of the Systems Gravitational Field - Particle

Quantization of the gravitational waves we shall carry out by quantization of the volumetric density of action in space of the generalized coordinates:

where R there is a scalar curvature of a space-time, ρ - mass density of a particle in a field, ρ_0 - mass density of a rest particle, φ_g - gravitational potential of a field.

Lagrangian to the Lagrange's equation submits which looks like:

$$\frac{d}{dt} \left(\frac{\partial l}{\partial \dot{q}} \right) = \frac{\partial l}{\partial q}. \quad (19)$$

For the generalized velocity we use size:

$$\dot{q} = \sqrt{2T}. \quad (20)$$

In this case the known formula for volumetric density of energy is correct:

owing to $\frac{\partial l}{\partial T} = 1$.

From formulas (17) and (20) follows that volumetric density of a particle kinetic and potential energy in a gravitational field is equal:

$$T = \frac{\dot{\mathbf{q}}^2}{2} = (\rho - \rho_0)c^2, \quad U = \rho\varphi_g - l_g. \quad (22)$$

Thus both components of volumetric density of action depend on a body density which creates curvature of a space-time.

Therefore in the Einstein's equation (11) the right part of the equation dependent on mass creating a gravitational field should be subject to quantization only. The time is not quantized value. Apparently are not quantized all parameters of a space-time (scalar curvature, metric tensor, Ricci's tensor, etc.). To quantization can be subject to only energy-impulse tensor.

Having substituted (22) in (19) with the account $l = T - U$, we shall receive in the left part of the equation (19):

$$\frac{d}{dt} \left(\frac{\partial l}{\partial \dot{\mathbf{q}}} \right) = \frac{d\dot{\mathbf{q}}}{dt} = \ddot{\mathbf{q}} = \rho \mathbf{a}, \quad (23)$$

where \mathbf{a} there is acceleration of a particle movement.

The right part of the equation (19) will be transformed to a kind:

$$\frac{\partial l}{\partial \mathbf{q}} = -\frac{\partial(\rho\varphi_g)}{\partial \mathbf{q}} + \frac{\partial l_g}{\partial \mathbf{q}} = \mathbf{f} + \frac{\partial l_g}{\partial \mathbf{q}}, \quad (24)$$

where $\mathbf{f} = -\frac{\partial(\rho\varphi_g)}{\partial \mathbf{q}}$ there is volumetric density of the gravitational force working on a particle from the other bodies.

At use (18) we find that size

$$\mathbf{f}_g = \frac{\partial l_g}{\partial \mathbf{q}} = \frac{c^4}{16\pi k} \frac{\partial R}{\partial \mathbf{q}} \quad (25)$$

there is a volumetric density of the force working on a particle owing to the Riemann's space-time curvature R .

V. GRAVITON ENERGY AND QUANTUM GRAVITATIONAL EIKONAL

The quantum of a gravitational field – a graviton as the quantum effect of gravitational radiation can be propagated far from massive bodies. It creates a curvature of the Riemann's spaces-time. Therefore a graviton has mass. The graviton mass is equal:

$$m = \frac{E}{c^2}, \quad (26)$$

where E there is a graviton energy, c – a light velocity.

Trace T an energy–impulse tensor in Einstein's equation is connected to scalar curvature of space-time R a ratio (14).

If the graviton is propagated in a direction of an axis X_1 the diagonal components of a metric tensor wave fluctuations owing to the cross-section of gravitational waves following: $h_{11} = 0$, $h_{22} = -h_{33}$ [10]. The same ratio of components should be in the energy-impulse tensor of a graviton (12). Therefore a trace of a graviton energy-impulse tensor is equal:

$$T = T_{00} = \frac{m}{V} c^2 = \frac{E}{V}, \quad (27)$$

where V there is normalizing volume. According to (14) the scalar curvature of space-time is equal:

$$R = -\frac{8\pi k}{c^4} \frac{E}{V}, \quad (28)$$

The action of a gravitational field is equal [6]:

$$S = \int l_g \sqrt{-g} d\Omega = \int l_g \sqrt{-g} dV d(ct), \quad (29)$$

where $d\Omega = dV d(ct)$ there is an element of a space-time volume. The size $\sqrt{-g}$ owing to its small size due to a graviton we believe to equal unit. At use of the space-time volume as $d\Omega = dV d(ct)$ the Lagrangian of a gravitational field as against (18) it is necessary to use as

$$l_g = \frac{c^3}{16\pi k} R.$$

Substituting this formula in (29) and assuming approximately constancy of scalar curvature in area of a graviton we shall find:

$$S = \int l_g dV d(ct) = \frac{c^4}{16\pi k} VRt + C, \quad (30)$$

where C there is a constant of integration which can depend from X_1 .

Substituting (28) in (30) we have:

$$S = -\frac{1}{2}Et + C. \quad (31)$$

Further to similarly electromagnetic field, see (7), we shall enter into consideration the concept of a quantum gravitational eikonal $S = \hbar\phi$ where \hbar there is Planck's reduced constant, $\phi = rX_1 - \omega t$ - its phase, r - wave number of a graviton, ω - its own frequency. We assume function of the quantum gravitational eikonal $S(X_1, t)$ approximately linear in a weak gravitational field [6, 11]. We shall note equivalence of quantum gravitational eikonal and actions of system a gravitational field - particle. Both sizes submit to a principle of a minimum (to Maupertuis' principle for action or Fermat's for eikonal) [6].

Equating a quantum gravitational eikonal and action we find:

$$S = \hbar\phi = \hbar(rX_1 - \omega t) = -\frac{1}{2}Et + C. \quad (32)$$

From the formula (32) follows that graviton energy is equal:

$$E = 2\hbar\omega, \quad (33)$$

and size $C = 2\hbar rX_1$. The spin of graviton it is $\pm 2\hbar$.

Energy of a relativistic mass particle is equal $E = \sqrt{p^2 c^2 + m_0^2 c^4}$. Therefore the formula (33) allows to assume that as against an ordinary particle the graviton rest mass is equal to zero $m_0 = 0$, and the impulse of the graviton is equal

$p = \frac{E}{c} = \frac{2\hbar\omega}{c} = 2\hbar r$. One of differences of a graviton from a photon consists that the photon mass is always equal to zero, and the graviton mass is equal to zero only rest. However as well as the photon the graviton cannot are in a condition of rest.

Having substituted (33) in (26) we find

$$m = \frac{E}{c^2} = \frac{2\hbar\omega}{c^2}$$

hence the mass of a graviton is proportional to its frequency. If for a graviton (by analogy to a photon) the rule of "red displacement" operates then at removal from massive bodies the graviton frequency, and hence its mass should decrease down to disappearance of the graviton (gravitonic darkness¹). At approach a graviton to the massive bodies the graviton frequency and its mass should increase.

If to accept for example the frequency of background thermal gravitational radiation $\omega = 1.26 \cdot 10^{12} s^{-1}$ [10] then graviton energy is $E = 2\hbar\omega = 2.66 \cdot 10^{-15} erg = 0,00166 eV$.

A graviton mass (26) of the background thermal gravitational radiations is $m = 2,96 \cdot 10^{-26} g$.

Propagation of a graviton passes in a direction of a normal to constant eikonal surface. Thus we have average radius of curvature of a constant eikonal surface (curvature of the Riemann's spaces) in the given approximation (a weak gravitational field) are much greater of a graviton wave lengths

$$\lambda = \frac{2\pi c}{\omega} \quad [11].$$

VI. THE QUANTUM FORM OF AN ENERGY-IMPULSE TENSOR

We shall consider the energy-impulse tensor (12) in more detail. It is supposed that into the energy-impulse tensor enters as making the stresses tensor:

¹ It is possible that in the Universe there are the vivid individuals seeing with the help of gravitons as well as Earth's individuals see with the help of photons.

$$\sigma_{ik} = \begin{pmatrix} T_{11} & T_{12} & T_{13} \\ T_{21} & T_{22} & T_{23} \\ T_{31} & T_{32} & T_{33} \end{pmatrix} = \begin{pmatrix} \sigma_X & \tau_{XY} & \tau_{XZ} \\ \tau_{YX} & \sigma_Y & \tau_{YZ} \\ \tau_{ZX} & \tau_{ZY} & \sigma_Z \end{pmatrix} \quad (34)$$

where T_{11}, T_{22}, T_{33} there are normal stresses, other components $\sigma_{ik} = T_{ik}$ for $i \neq k$ - tangential stresses. A component $T_{00} = \rho c^2$ - volumetric density of energy of a mass particle or graviton, T_{10}, T_{20}, T_{30} - components of the impulse density multiplied on light velocity c , T_{01}, T_{02}, T_{03} - components of the energy flux density divided on c .

In a basis of the further research we shall assume absence of a stresses state birth of empty space owing to its possible curvature.

In [12] it has been shown that in a fluid or gas there is an uncertainty of a sign on tangential stresses. Moreover the stresses tensor only approximately describes a stressed state of a fluid and gas. In a fluid and gas the stresses tensor is absent. For calculation of a fluid or gas flux it is necessary to use the vector formula connecting force $d\mathbf{F}$ and velocity \mathbf{V} as [12]:

$$d\mathbf{F} = \vec{\eta} dS \times \text{rot}\mathbf{V}, \quad (35)$$

$$dF_x \mathbf{i} + dF_y \mathbf{j} + dF_z \mathbf{k} = 2\eta \{ (dS_y \omega_z - dS_z \omega_y) \mathbf{i} + (dS_z \omega_x - dS_x \omega_z) \mathbf{j} + (dS_x \omega_y - dS_y \omega_x) \mathbf{k} \}, \quad (37)$$

where $\mathbf{i}, \mathbf{j}, \mathbf{k}$ there are in this case unit vectors of 3-dimensional space. Assuming space homogeneous we use a scalar variant viscosity tensor η .

At use of the formula (35) the uncertainty of the tangential stresses sign and some other problems connected with stresses tensor [12] on which we shall not stop disappear.

We shall write down the energy-impulse tensor (12) in the following kind:

where dS there is area of contacting layers in a fluid or gas, $\vec{\eta}$ - viscosity tensor of the second rank which diagonal components there are molecular viscosity and not diagonal components - turbulent viscosity.

If a flux of fluid or gas passes for example in a direction axes X the directions of vectors in the formula (35) are shown on fig. 1.

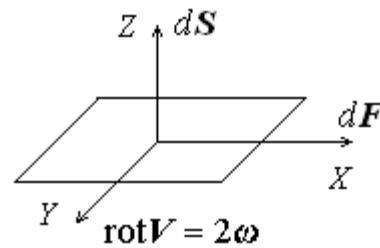


Figure 1: The directions of vectors in the formula (35)

For our purposes in the formula (35) using cyclic frequency of a medium rotation $\omega = \frac{1}{2} \text{rot}\mathbf{V}$ [13] therefore it is convenient to write down as:

$$d\mathbf{F} = 2\vec{\eta} dS \times \omega, \quad (36)$$

The scalar variant of the formula (36) looks like:

$$T_{ik} = \begin{pmatrix} \rho c^2 & T_{01} & T_{02} & T_{03} \\ T_{10} & \frac{dF_1}{dS_1} & \frac{dF_2}{dS_1} & \frac{dF_3}{dS_1} \\ T_{20} & \frac{dF_1}{dS_2} & \frac{dF_2}{dS_2} & \frac{dF_3}{dS_2} \\ T_{30} & \frac{dF_1}{dS_3} & \frac{dF_2}{dS_3} & \frac{dF_3}{dS_3} \end{pmatrix}, \quad (38)$$

where transition to digital indexes is carried out. Taking into account (37), we have:

$$T_{ik} = \begin{pmatrix} \rho c^2 & T_{01} & T_{02} & T_{03} \\ T_{10} & \frac{2\eta(dS_2\omega_3 - dS_3\omega_2)}{dS_1} & \frac{2\eta(dS_3\omega_1 - dS_1\omega_3)}{dS_1} & \frac{2\eta(dS_1\omega_2 - dS_2\omega_1)}{dS_1} \\ T_{20} & \frac{2\eta(dS_2\omega_3 - dS_3\omega_2)}{dS_2} & \frac{2\eta(dS_3\omega_1 - dS_1\omega_3)}{dS_2} & \frac{2\eta(dS_1\omega_2 - dS_2\omega_1)}{dS_2} \\ T_{30} & \frac{2\eta(dS_2\omega_3 - dS_3\omega_2)}{dS_3} & \frac{2\eta(dS_3\omega_1 - dS_1\omega_3)}{dS_3} & \frac{2\eta(dS_1\omega_2 - dS_2\omega_1)}{dS_3} \end{pmatrix}. \quad (39)$$

The tensor (39) is an energy-impulse tensor creating a curvature of a space - time. For quantization of the energy-impulse tensor first of all the size η should be expressed through the

size η we use it Planck's value $\eta = \frac{\hbar}{V}$ where V there is normalizing volume. Besides there are no reasons to assume the areas in (36) various therefore shall accept $dS_1 = dS_2 = dS_3$. In this case the tensor (39) it will be transformed to a kind:

Planck's sizes: Planck's length $\left(\frac{\hbar k}{c^3}\right)^{\frac{1}{2}}$, Planck's time $\left(\frac{\hbar k}{c^5}\right)^{\frac{1}{2}}$ and Planck's mass $\left(\frac{\hbar c}{k}\right)^{\frac{1}{2}}$. Instead of

$$T_{ik} = \begin{pmatrix} \rho c^2 & T_{01} & T_{02} & T_{03} \\ T_{10} & \frac{2\hbar(\omega_3 - \omega_2)}{V} & \frac{2\hbar(\omega_1 - \omega_3)}{V} & \frac{2\hbar(\omega_2 - \omega_1)}{V} \\ T_{20} & \frac{2\hbar(\omega_3 - \omega_2)}{V} & \frac{2\hbar(\omega_1 - \omega_3)}{V} & \frac{2\hbar(\omega_2 - \omega_1)}{V} \\ T_{30} & \frac{2\hbar(\omega_3 - \omega_2)}{V} & \frac{2\hbar(\omega_1 - \omega_3)}{V} & \frac{2\hbar(\omega_2 - \omega_1)}{V} \end{pmatrix}. \quad (40)$$

Let's consider for example the energy-impulse tensor for propagation of gravitational radiation to a direction of axis X_1 . Gravitational waves are cross-section hence the vector of frequency is directed along an axis X_1 . In this case the formula (40) looks like:

In the tensor of energy-impulse the components $\pm \frac{2\hbar\omega_1}{V} = \pm \varepsilon$ enter which characterize volumetric density of energy of gravitational radiation quantum - graviton. Two signs of the spin are reflect two directions of polarization: (plus) a vector of cyclic frequency ω_1 is directed along direction of a graviton propagation and (minus) against direction of a graviton propagation.

$$T_{ik} = \begin{pmatrix} \rho c^2 & T_{01} & T_{02} & T_{03} \\ T_{10} & 0 & \frac{2\hbar\omega_1}{V} & -\frac{2\hbar\omega_1}{V} \\ T_{20} & 0 & \frac{2\hbar\omega_1}{V} & -\frac{2\hbar\omega_1}{V} \\ T_{30} & 0 & \frac{2\hbar\omega_1}{V} & -\frac{2\hbar\omega_1}{V} \end{pmatrix}. \quad (41)$$

Asymmetry of the energy-impulse tensor T_{ik} is connected with basic refusal from use symmetric stress tensor [12].

In spite of the fact that we have entered the graviton energy in energy-impulse tensor it does not mean that tensor began to have quantum character. Further it is necessary to take into account ideas of the quantum mechanics matrix form and to add at least to tensor components with graviton energy a factor $\exp\left(\frac{i}{\hbar}S\right) = \exp i(rX_1 - \omega_1 t)$ [14] where $S = \hbar\phi$ is a quantum of gravitational eikonal (32), $\phi = rX_1 - \omega_1 t$ - its phase. We assume function of a

gravitational eikonal quantum $S(X_1, t)$ approximately linear in a weak gravitational field. In the matrix form of quantum mechanics ω_1 carries the name of spectral frequency and characterizes transition of system from one quantum state in another. The factor $\exp\left(\frac{i}{\hbar} S\right)$

characterizes transition of a gravitational field quantum (graviton) on quantum states in a space-time. We shall note that at record of matrixes in the matrix form of quantum mechanics the exponential factors at a component of matrix frequently omit [14]. Thus the energy-impulse tensor will receive a kind:

$$T_{ik} = \begin{pmatrix} \rho c^2 & T_{01} & T_{02} & T_{03} \\ T_{10} & 0 & \varepsilon \exp\left(\frac{i}{\hbar} S\right) & -\varepsilon \exp\left(\frac{i}{\hbar} S\right) \\ T_{20} & 0 & \varepsilon \exp\left(\frac{i}{\hbar} S\right) & -\varepsilon \exp\left(\frac{i}{\hbar} S\right) \\ T_{30} & 0 & \varepsilon \exp\left(\frac{i}{\hbar} S\right) & -\varepsilon \exp\left(\frac{i}{\hbar} S\right) \end{pmatrix} = \begin{pmatrix} \rho c^2 & T_{01} & T_{02} & T_{03} \\ T_{10} & 0 & \frac{2\hbar\omega_1}{V} \exp i(rX_1 - \omega_1 t) & -\frac{2\hbar\omega_1}{V} \exp i(rX_1 - \omega_1 t) \\ T_{20} & 0 & \frac{2\hbar\omega_1}{V} \exp i(rX_1 - \omega_1 t) & -\frac{2\hbar\omega_1}{V} \exp i(rX_1 - \omega_1 t) \\ T_{30} & 0 & \frac{2\hbar\omega_1}{V} \exp i(rX_1 - \omega_1 t) & -\frac{2\hbar\omega_1}{V} \exp i(rX_1 - \omega_1 t) \end{pmatrix}. \quad (42)$$

The energy-impulse tensor (42) has quantum character.

VII. THE GRAVITON EQUATION

For a finding of the graviton equation we shall substitute an energy-impulse tensor (42) in Einstein's equation as (15). The tensor energy-impulse trace (42) looks like $T = \rho c^2$. Hence the equation (15) - the graviton equation will be transformed to a kind:

$$R_{ik} = \frac{8\pi k}{c^4} \left(T_{ik} - \frac{1}{2} g_{ik} \rho c^2 \right). \quad (43)$$

Let's consider the graviton equation in almost flat space at absence of a mass component in energy-impulse tensor (42) i.e. at $T = \rho c^2 = 0$. The gravitons practically do not bend space-time. Therefore it is possible to use the formula for wave fluctuations of metric tensor h_{ik} as [6]:

$$\frac{\partial^2 h_{ik}}{\partial X_\alpha \partial X_\alpha} - \frac{1}{c^2} \frac{\partial^2 h_{ik}}{\partial t^2} = \frac{16\pi k}{c^4} T_{ik}. \quad (44)$$

The graviton radiation cross-section therefore all tensor components h_{ik} in the equation (44) with indexes 1 at the propagation of graviton in direction X_1 are excluded. Tensor components h_{ik} remain only: h_{23} and $h_{22} = -h_{33}$ [10]. We shall notice also that in the energy-impulse tensor (42) $T_{22} = -T_{33}$.

For a component h_{23} the wave equation (44) looks like:

$$\frac{\partial^2 h_{23}}{\partial X_1^2} - \frac{1}{c^2} \frac{\partial^2 h_{23}}{\partial t^2} = -\frac{16\pi k}{c^4} \frac{2\hbar\omega}{V} \exp i(rX_1 - \omega t). \quad (45)$$

For component h_{22} a sign in the right part of the equation is positive, and for component h_{33} is negative. The index 1 at frequency is omitted. Therefore designating $\chi = h_{ik} V$ where $ik = 22, 23, 33$ we shall find:

$$\frac{\partial^2 \chi}{\partial X_1^2} - \frac{1}{c^2} \frac{\partial^2 \chi}{\partial t^2} = \pm \frac{32\pi k \hbar \omega}{c^4} \exp i(rX_1 - \omega t). \quad (46)$$

The factor before an exponent in the right part (46) is proportional to the double scalar curvature of space-time (28) due to presence graviton, $R = \frac{8\pi k}{c^4} \frac{E}{V} = \frac{8\pi k}{c^4} \frac{2h\omega}{V}$. This factor is extremely small $\frac{32\pi k h}{c^4} = 0,87 \cdot 10^{-74} \text{ cm} \cdot \text{s}$ that specifies almost flat space-time.

The equation (46) describes a gravitational wave and graviton propagating from left to right therefore the general solution of this equation we shall search as:

$$\chi = C_1 f_1(rX_1 - \delta t) + C_2 f_2(t) \exp i r X_1, \quad (47)$$

where C_1 and C_2 there are constants, $f_1(rX_1 - \delta t)$ and $f_2(t)$ - any functions, δ - gravitational wave frequency connected with a velocity of its propagation $r = \frac{\delta}{c}$. Frequency δ is not equal to own graviton frequency ω which can belong to other wave. The first term (47) describes the gravitational wave the second term - graviton. Let's substitute (47) in the equation (46) which have been written down as:

$$\frac{\partial^2 \chi}{\partial X_1^2} - \frac{1}{c^2} \frac{\partial^2 \chi}{\partial t^2} = \pm \gamma \omega \exp i(rX_1 - \omega t), \quad (48)$$

$$\begin{aligned} h_{ik} &= a e_{ik} \cos(rX_1 - \delta t) \mp \frac{32\pi k h \omega e_{ik}}{c^2(\delta^2 - \omega^2)V} \exp i(rX_1 - \omega t) = \\ &= a e_{ik} \cos(rX_1 - \delta t) \mp \left(\frac{2Rc^2 e_{ik}}{(\delta^2 - \omega^2)} \right) \exp i(rX_1 - \omega t) \end{aligned}, \quad (53)$$

where a there is an amplitude of a wave, \mathbf{r} - a wave vector (of a wave and graviton) in a direction of a wave propagation. The value e_{ik} there is a unit polarization tensor (of a wave and graviton) obeying the conditions [15]:

$$e_{ik} = e_{ki}, \quad e_{ii} = 0, \quad k_i e_{ik} = 0, \quad e_{ik} e_{ik} = 1. \quad (54)$$

The first term (53) characterizes propagation of the gravitational wave the second term - graviton. As against an electromagnetic wave which polarization is determined by a vector of the electric field oscillations, the polarization of a gravitational wave (and graviton) has essentially

where it is designated $\gamma = \frac{32\pi k h}{c^4}$ - a constant.

The first term (47) satisfies to the equation (48) without the right part. Therefore after substitution we shall find:

$$S \frac{d^2 f_2}{dt^2} + \delta^2 f_2 \pm \frac{\gamma \omega c^2}{C_2} \exp(-i\omega t) = 0. \quad (49)$$

The particular solution of the equation (49) dependent on own graviton frequency ω we shall search as:

$$f_2 = A \exp(-i\omega t). \quad (50)$$

Substituting (50) in (49) we shall find:

$$A = \pm \frac{\gamma \omega c^2}{C_2(\omega^2 - \delta^2)}. \quad (51)$$

Hence according to (47) the solution of the equation (48) looks like:

$$\chi = C_1 f(rX_1 - \delta t) \pm \frac{\gamma \omega c^2}{(\omega^2 - \delta^2)} \exp i(rX_1 - \omega t). \quad (52)$$

Taking into account a designation $\chi = h_{ik} \mathbf{V}$ where $ik = 22, 23, 33$, and also $\gamma = \frac{32\pi k h}{c^4}$, and (28) we shall find:

tensor character. The third condition (54) is a condition of the gravitational waves (and graviton) cross-section.

The top sign (52) and (53) corresponds to size h_{22} , and the bottom sign h_{23} and h_{33} . The size h_{ik} naturally does not depend on normalizing volume V .

VIII. REGISTRATION OF GRAVITON

The kind of function (53) allows draw the some conclusions. Far from massive bodies a graviton as the quantum effect is practically imperceptible.

It practically has not influence on registration of the gravitational waves.

However function (53) has interesting feature. At $\omega \rightarrow \delta$ i.e. at aspiration of a graviton own frequency to the gravitational wave frequency fluctuation components of the metric tensor h_{ik}

aspire to infinity. The resonance of the gravitational wave frequency and graviton own frequency which is in structure of other wave is observed. This phenomenon can be used for registration of gravitons.

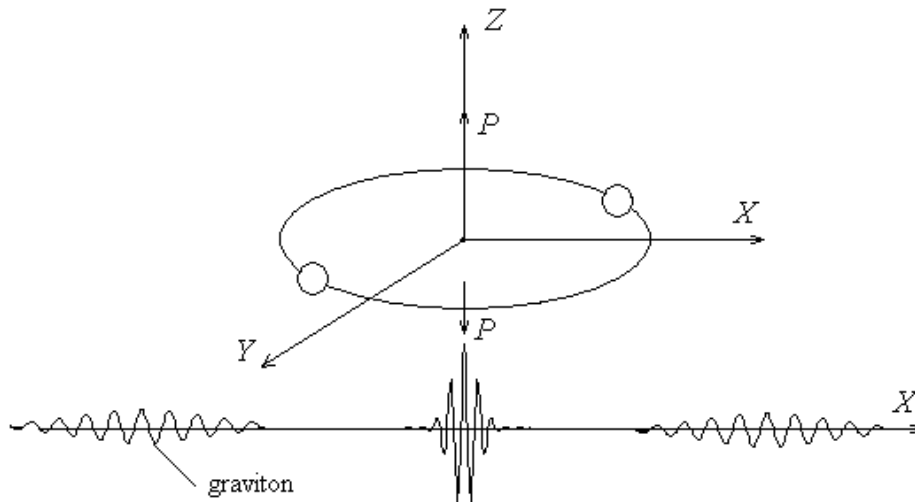


Figure 2: Double star radiating the gravitational waves and a graviton flying in the field of a double star

Let's assume that two massive cosmic bodies, fig. 2, (for example a double star) rotate around of the common mass centre. This system radiates the flux P of the gravitational waves $h_{ik} = ae_{ik} \cos(rX_1 - \delta t)$ with constant frequency δ . If graviton as quantum phenomenon of another wave gets in area of such cosmic bodies its own frequency ω grows according to the formula similar (6) similar photon frequency. According to the formula (53) growth of a graviton energy occurs much faster $2\hbar\omega$ that specifies resonant pumping of energy of these massive bodies gravitational field in a graviton. Energy of a graviton ω become very big and graviton can be registered. Probably for this purpose it is necessary to install the detector on massive bodies or near to them (on their planet or the artificial satellite). With the help of such detector it is possible to register abnormal splash in gravitation at graviton passage.

At distance from the bodies a graviton return the energy to a gravitational field of the bodies; its frequency falls (as red displacement in gravitation). Therefore energy of a gravitational field of the massive bodies does not change at

flight near them of gravitons. We shall notice also that Riemann's curvature of space-time is positive therefore in the considered effect the fluctuation components of metric tensor h_{23} and h_{33} take part only. They resonantly grow at flight of a graviton near the massive bodies.

IX. CONCLUSION

On the basis of Einstein's equation for gravitation the gravitational radiation of the massive bodies as a double star is investigated. By refusal from a stresses tensor into energy-impulse tensor, and replacement corresponding a component in power sizes also introductions of a gravitational eikonal quantum the quantization of gravitational radiation is lead.

The solution of the quantum equation of Einstein in the certain direction shows that this solution represents the sum of two composed, first of which characterizes gravitational waves, and the second - graviton.

At approach of the gravitons to a double star there is a resonant pumping of the gravitational field energy to gravitons. It allows register the

gravitons. At distance of the gravitons from a double star their energy comes back in a gravitational field of the stars. Frequency of the gravitons decreases as red displacement for gravitation. Therefore as a whole the gravitons as quantum phenomenon do not influence on a gravitational field of stars.

14. Mott N., Sneddon I. *Wave Mechanics and its Applications*. Moscow: ComKniga, 2007, p. 389.
15. Peters P.C., Mathews J. *Gravitational Radiation from Point Masses in a Keplerian Orbit*. *Phys. Rev. V.* 131, No. 1, 1963, pp. 435 – 440.

REFERENCES

1. Bronstein M.P. *Quantization of Gravitational Waves*. Moscow, JETP, No. 6, 1936, pp. 195 - 236.
2. Wheeler J.A. *Geons*. *Phys. Rev. V.* 97, 1955, pp. 511 – 536.
3. Kiefer C. *Quantum Gravity*. New York: Oxford Univ. Press, 2004. 308 p.
4. Rubakov V.A., Tinyakov P.G. *Infrared – modified Gravities and Massive Gravitons*. Moscow. *Uspekhi Fizicheskikh Nauk. V.* 178, No. 8, 2008, pp. 785 – 822.
5. Christian Corda. *Interferometric Detection of Gravitational Waves: the Definitive Test for General Relativity*. *Int. J. of Modern Physics D*. Vol. 18, No. 14, 2009, pp. 2275-2282.
6. Landau L.D., Lifshits E.M.. *Theory of Field*. Moscow: Science, 1967. 460 p.
7. Kaluza T. *To Problem of Physics unity, The Collection: Albert Einstein and the Theory of Gravitation*, Moscow, World, 1979, pp. 529-534.
8. Kris Pardo, Maya Fishbach, Daniel E. Holz, David N. Spergel. *Limits on the Number Spacetime Dimensions from GW170817*. *ArXiv.org 1801.08160v1*, 24 Jan 2018, pp. 1-7.
9. Fradkin E.S. *The Method of Green's Function in the Theory of the Quantum Fields and Quantum Statistics*, Moscow, Works FIAN, Science, V. 29, 1965, pp. 7-138.
10. Zeldovich J.B., Novikov I.D. *The Theory of Gravitation and Evolution of Stars*, Moscow, Science, 1971. 484 p.
11. Levich V.G., Vdovin J.A., Mjamlin V.A. *Theoretic Physics Course. V. 2*. Moscow: FIZMATGIS, 1962. 820 p.
12. Volobuev A.N. *Basis of Nonsymmetrical Hydromechanics*. New York. Published by Nova Science Publishers, Inc. 2012. 198 p.
13. Schlichting H. *The Boundary Layer Theory*. Moscow: Science, 1974, p. 63.



Scan to know paper details and
author's profile

Benefits of Precision Agriculture in Nigeria

Abdulsalam Abdulwaheed

ABSTRACT

This study was carried out in National Centre for Agricultural Mechanization (NCAM) situated at Ifelodun Local Government Area (LGA) of Kwara State, Nigeria. The research work examines Precision Agriculture concept in agricultural production which is becoming an attractive idea in managing natural resources and realizing modern sustainable development of agriculture based on information technology (IT). It includes technologies such as Geographic Information System (GIS), Satellite Remote Sensing and Global Positioning System (GPS). And it also brings agriculture into digital age. With the latest take-off of the NigeriaSat-1, an earth observing satellite for the meteorological, natural resources, hazard observation and management purposes, Nigeria now joins the league of nations that have access to the opportunities afforded by Satellite Remote Sensing in revolutionizing their agriculture. The market for precision farming therefore is of significant economic importance and offers great opportunities for local farmers in both “pre” and “post” farming seasons. The study was therefore carried out to review the meaning of precision agriculture, highlights its components and describes how Nigerian farmers can harness them for large scale agricultural production.

Keywords: precision agriculture; gps; nigeria.

Classification: FOR code: 099901

Language: English



London
Journals Press

LJP Copyright ID: 925643
Print ISSN: 2631-8490
Online ISSN: 2631-8504

London Journal of Research in Science: Natural and Formal

Volume 19 | Issue 2 | Compilation 1.0



Benefits of Precision Agriculture in Nigeria

Abdulsalam Abdulwaheed

ABSTRACT

This study was carried out in National Centre for Agricultural Mechanization (NCAM) situated at Ifelodun Local Government Area (LGA) of Kwara State, Nigeria. The research work examines Precision Agriculture concept in agricultural production which is becoming an attractive idea in managing natural resources and realizing modern sustainable development of agriculture based on information technology (IT). It includes technologies such as Geographic Information System (GIS), Satellite Remote Sensing and Global Positioning System (GPS). And it also brings agriculture into digital age. With the latest take-off of the NigeriaSat-1, an earth observing satellite for the meteorological, natural resources, hazard observation and management purposes, Nigeria now joins the league of nations that have access to the opportunities afforded by Satellite Remote Sensing in revolutionizing their agriculture. The market for precision farming therefore is of significant economic importance and offers great opportunities for local farmers in both “pre” and “post” farming seasons. The study was therefore carried out to review the meaning of precision agriculture, highlights its components and describes how Nigerian farmers can harness them for large scale agricultural production.

Keywords: precision agriculture; gps; nigeria.

Author: National Centre for Agricultural Mechanization (NCAM) KM 20, Ilorin – Lokoja Highway, Idofian, Kwara State, Nigeria.

I. INTRODUCTION

The National Centre for Agricultural Mechanization was established, formally by the

Decree No. 35 of 1990 with the mandate to accelerate the positive transformation of the agricultural sector of the Nigerian economy in order to increase the quality and quantity of agricultural products. This mandate is being achieved through adoptive and innovative research and development activities which include:

- i. To encourage and engage in adaptive and innovative research towards the development of indigenous machine for farming and processing techniques;
- ii. To design and develop simple and low-cost equipment which can be manufactured with local materials, skill and facilities;
- iii. To standardize and certify in collaboration with the Standards Organization of Nigeria (SON), agricultural machines, equipment and engineering practices in use in Nigeria;
- iv. To bring into focus mechanical technologies and equipment developed by various institutions, agencies or bodies and evaluate their suitability for adoption;
- v. To disseminate information on methods and programmes for achieving speedy agricultural mechanization;
- vi. To provide training facilities by organizing courses and seminars specially designed to ensure sufficiently trained manpower for appropriate mechanization;
- vii. To promote co-operation in agricultural mechanization with similar institutions in Nigeria, and with international bodies connected with agricultural mechanization.

A very critical mandate of NCAM is to ensure the availability of sufficiently trained manpower for

appropriate mechanization of Nigeria's agriculture. This has made the Centre to establish an Agro-metrological unit of National Centre for Agricultural Mechanization (NCAM) related to major technologies of Precision Agriculture in which an agricultural mechanization method which depends strongly on electronics, ITs and communications, and also requires technical skill and manpower for plant and animal production respectively.

The way manufacturing has changed completely in the last two centuries, farming has also changed. The classic picture of the farmer one of bucolic simplicity is wildly out of date. Technology, cost and economies of scale have driven commercial farmers around the world to change, and precision farming is beginning to gain popularity (Doug et al, 2003).

Precision agriculture is an agricultural mechanization method which depends strongly on electronics, ITs and communications, and also requires technical skill and manpower for plant and animal production that are site-specific and animal-specific respectively (Asoegwu, 2007). 1990 assessments indicated that 82 million hectares out of Nigeria's total land area of about 91 million hectares were arable, however only about 34 million hectares were being cultivated on a small scale. Big scale and export (or revenue generation) oriented agriculture have suffered countless setback in recent times. With the renew quest of the Federal and some State governments into the development of large scale agriculture and mechanized farming in order to shore up food security and foreign exchange earnings, there is need for adoption of uses of technologies of Precision Agriculture, which offer a wide range of applications in order to effectively harness human, natural and man-made resources for sustainable agricultural production and improved crop yields in Nigeria (T'Miebaka, 2004).

Along with GIS, Remote Sensing and GPS, which are major technologies of precision Agriculture, there have appeared a wide range of sensors,

monitors and controllers for agricultural equipment such as shaft monitors, pressure transducers and servomotors. Together they will enable commercial farmers in Nigeria to use electronic guidance aids to direct equipment movements such as combine harvester more accurately, provide precise positioning of all equipment actions and chemical applications and analyse all of that data in association with other sources of data (agronomic, climatic, etc), this add up to a new and powerful toolbox of management tools for the progressive farm manager.

Therefore, this study was carried out to review the meaning of precision agriculture, highlights its components and describes how Nigeria farmers can harness them for large scale agricultural production.

II. WHAT IS PRECISION AGRICULTURE?

Gary (2004) defined Precision Agriculture as a comprehensive system designed to optimize agricultural production through the application of crop information, advanced technology and management practices. Precision agriculture requires integration of three elements: (1) positioning capabilities (currently, global positioning system or GPS) to know where equipment is located; (2) real-time mechanisms for controlling nutrient, pesticide, seed, water or other crop production inputs; and (3) databases or sensors that provide information needed to develop input response to site-specific conditions (Karlen et al, 1998). Intensive soil investigation is carried out using the global positioning system (GPS) consisting of 24 satellites that transmits signals picked up by the user receivers. The use of GPS allows soil sample sites to be accurately located within a field and fertility levels mapped. This technology also allows yield samples to be taken from accurately located positions and then compared to soil test results. Using this technology, producers can pinpoint locations of significant soil variability for example, in terms of fertility level. Fertilizer applicators can then be used to apply fertilizers at variable rates using the

technology characteristics of the soil at different locations, these data are plotted onto maps corresponding to each location for application of farm inputs such as fertilizer, pesticide and water of remote sensing according to variations in fertility levels. The combination of variable fertilizer applications and yield monitoring can lead to better understanding of variability within a field. The objective would be to reduce that variability, thus increasing yields.

Precision agriculture also involves the determination of physical, chemical and biological components within fields in ways that optimizes farm returns and minimizes chemical and environmental hazards (T'Miebaka, 2004).

III. GOAL AND OBJECTIVES OF PRECISION AGRICULTURE

The goal of precision farming is to gather and analyse information about the variability of soil and crop conditions in order to maximize the efficiency of crop inputs within small areas of the farm field. To meet this efficiency goal, the variability within the field must be controllable. Efficiency in the use of crop inputs means that fewer crop inputs such as fertilizer and chemicals will be used and placed where needed. The benefits from this efficiency will be both economic and environmental. Environmental costs are difficult to quantify in monetary terms. The reduction of soil and groundwater pollution from farming activities has a desirable benefit to the farmer and to society (Gary, 2004).

IV. HOW DOES A FARMER GET STARTED IN PRECISION AGRICULTURE?

In order for a farmer to get started, he has to understand the three key elements on which precision agriculture rely i.e. Information, Technology and Management.

Information is perhaps the modern farmer's most valuable resource. Timely and accurate information is essential in all phases of production from planning through post-harvest (Gary, 2004). Information available to the farmer

includes crop characteristics, soil properties, fertility requirements, weed populations, insect populations, plant growth response, harvest data, and post-harvest processing data. The precision farmer must seek out and use the information available at each step in the system.

Modern technology in agriculture is the second key to success in Precision Agriculture. Technology is rapidly evolving and the farmer must keep up with the changes that may be of benefit in his or her operation. The personal computer is one example of such technology. The computer can help the farmer organise and manage data more effectively. Computer software, including spreadsheets, databases, geographic information systems (GIS) and other types of application software are readily available. The global positioning system (GPS) has given the farmer the means to locate position in the field to within a few feet. Sensors are available that can monitor soil properties, crop condition, harvesting, or post-harvest processing and give instant results or feedback which can be used to adjust or control the operation.

Management, the third key to success, combines the information obtained and the available technology into a comprehensive system. Without the proper management, precision crop production would not be effective. Farmers must know how to interpret the information available, how to utilize the technology, and how to make sound production decisions.

V. PRECISION AGRICULTURE: KEY TECHNOLOGIES & CONCEPTS REQUIRED

The tools required for effective Practicing Agriculture include:

- i. Yield Monitors: These are crop yield measuring devices installed on harvesting equipment. They have the capability of indicating yield (kg/ha), total kg, ha/hour, hectare worked, grain moisture content, etc. They provide information on crop yield at regular intervals by time or distance (e. g.

- every second or every few metre). The yield data from the monitor is recorded and stored at regular intervals along with positional data received from the GPS unit. GIS software takes the yield data and produces the yield maps.
- ii. Global Positioning System (GPS): GPS is a network of 24 satellites orbiting the earth which transmit precise satellite time and location information to ground receivers. It is used to pinpoint the location (geo-reference) of yield data collected, and provide accuracy of one to three meters.
 - iii. The ground receiving units are able to receive this location information from several satellites at a time for use in calculating a triangulation fix thus determining the exact location of the receiver. This is used to produce yield maps for each field.
 - iv. Geographical Information System (GIS): this consist of a computer software database system used to input, store, retrieve, analyse and display, in map-like form, spatially referenced geographical information such as data from GPS and Yield Monitors.
 - v. Variable Rate Technology (VRT): This consists of farm field equipment such sprayer and planter with the ability to precisely control the rate of application of crop inputs and tillage operations. For example, a fertilizer applicator with VRT provide a means of assuring that fertilizer applications are made only in amounts and locations where they are needed. The basic logic of VRT fertilizer application is to optimise application of fertilizer in areas of high productivity and increase fertilizer application to area of low productivity.
 - vi. Remote Sensors: This equipment produces image data from the soil and crops and this data is processed and then added to the GIS database.
 - vii. Computer Hardware and Software: Computer support is required to analyse the data collected by yield monitors and GPS,

this will be supplied in readable formats such as maps, graphs, charts or reports.

5.1 Method of approach

To practise precision agriculture, farmers must select and use the necessary equipment and technology. By selecting equipment capable of high accuracy application, the farmer has achieved the first step in implementing precision agriculture. The same is true in planting, tillage, harvesting and post-harvest equipment decisions. With this background in mind, comprehensive precision agriculture system can be viewed in two phases: Site specific management and Postharvest process control.

Site specific management is the field phase of the production system. Once the necessary equipment and technology are in place, the farmer can decide to continue to manage the fields by a site specific approach. In site specific management, the field is broken down into smaller grids and decisions are based on the requirements of each grid. GPS/GIS technology and variable rate equipment are used to apply inputs based on the grid requirements. By treating each grid according to its prescription, over application of chemicals and seed are avoided on areas where it will do no good. Areas that require the higher rates can still receive them.

Post harvesting processing is the second phase of the comprehensive approach. By using sensors to monitor the postharvest process, computers can be used to enhance the quality of the product or reduce energy requirements. The best quality product can then be delivered to the consumers.

IV. BENEFITS OF PRECISION AGRICULTURE

Through precision agriculture an area of land within a field may be managed with different levels of input depending upon the yield potential of the crop in that particular area of land. Earl et al (1996) states that the benefits of precision farming are in two folds: (i) the cost of

producing the crop in an area of land can be reduced (ii) the risk of environmental pollution from agrochemicals applied at levels greater than those required by the crop can be reduced.

Precision agriculture is of immense benefits to farmers in the following ways:

1. Efficient use of equipment

Information on soil characteristics and weather can be used to plan and improve scheduling of operations, which can increase machinery utilization rates and lower per-acre costs. Also, GPS-based guidance systems can allow farm machinery operators to achieve greater field efficiency under difficult conditions. They can reduce overlap and missed applications of inputs (e.g. spraying), helping fatigued operators maintain higher field efficiency.

2. Risk reduction

At the field level, precision farming provides site-specific management that can point out problems with growing conditions, thereby reducing variability in net returns. At the farm level, precision farming information can be used to improve variety choice, crop rotation, and other agronomic practices that reduce risk. As well, information on crop growth during the season can help you make more informed market decisions.

3. Management of differentiated products

In the future, precision technology may help farmers differentiate their production within a particular field. For example, you might segregate higher protein wheat for marketing in more rewarding channels. In addition, precision farming technology will allow the additional control that is required when you are managing the production of differentiated products as opposed to the production of regular bulk crops. It will allow documentation of crops conditions and control of inputs to meet the very specific requirements of these crops.

4. Environmental stewardship

Precision application of chemical and fertilizer will better match crop requirements, and will prevent over-application, which can be non-beneficial to the environment. The management practices generated by precision farming technologies will promote good land stewardship.

VII. CONCLUSION

As growers adopt precision agriculture, new technologies will continue to emerge. The next big advancement will be the use of artificial intelligence. While AI will never be able to replicate the kind of complex decisions farmers are required to make on regular basis, it could very well be used to help make those decisions easier.

Today's farmers have access to a wealth of data. So much data, in fact, they often don't know what to do with it. AI has the capability of analyzing huge amounts of data in a short period and using it to suggest the best course of action. This information could then be used to predict the best time to plant, to predict the outbreaks of pests and disease before they occur, and to offer in-field inventory management that could offer yield predictions prior to harvest.

I hope this provides some insight into precision agriculture today and the continued important role it will play in the future. Expect industry and technology companies to continue to explore the possibilities posed by the marriage of technology with the needs of the ag producers to produce enough food to feed the world's projected 9 billion people by 2050.

REFERENCES

1. Aseogwu, S. and Aseogwu, A. (2007): "An Overview of Agricultural Mechanisation and its Environmental Management in Nigeria". *Agricultural Engineering International: the*

- CIGR Ejournal. Invited Overview No. 6. Vol. IX. May, 2007 (Online). [http://cigr-ejournal.tamu.edu/submissions/volume9/Invited%20overview%Aseogwu%%203 May 2007.pdf](http://cigr-ejournal.tamu.edu/submissions/volume9/Invited%20overview%Aseogwu%%203%20May%202007.pdf)
2. Doug, R., Luvall, J. C., Shaw, J., Mask, P., Kissel, D., and Sullivan, D (2003): Precision Agriculture: Changing the Face of Fanning. Geotimes, USA (Online). http://www.geotimes.org/nov03/features_h tm1
 3. Earl, Wheeler, Blackmore (1997): Precision Farming - The Management of Variability. The Journal of the Institution of Agricultural Engineers, Landwards, Vol. No. 4 ppl8-23, July 16, 1997 (Online). http://www.silsoecranfield.ac.uk/cpf/papers /landwards/LANDW-P_FinalF.htm
 4. Gary, T. R. (2004): Precision Agriculture: A Comprehensive Approach (Online). <http://www.bae.ncsu.edu/programs/extensi on/agmachine/precision/>
 5. Le Meridien, Abuja, June 15-17, 2004 (Online). <http://www.nasrda.org/docs/opti mising.pdf>
 6. Karlen, D. L., S. S. Andrews, T. S. Colvin, D. B. Jaynes and E. C. Berry (1998); Spatial and
 7. Temporal Variability in Corn Growth, Development, Insect Pressure, and Yield. In P.
 8. C. Robert et al. (ed). Proceedings of 4th International Conference on Precision Agriculture. American Society of Agronomy. Madison, WI T'M biebaka Iyalla (2004): Optimising Agricultural Yields in Nigeria Using Remote Sensing, Global Positioning System (GPS) and Geographic Information System (GIS).
 9. Technology. A paper presented to the National Workshop on NigeriaSat-1 and GIS,



Scan to know paper details and
author's profile

Ion Potential Principle Summary

Wang Hai-Jun

ABSTRACT

In this paper, in addition to the ionic potential of the meaning, influencing factors, variation, polarizability and the relationship of extensive and in-depth discussion, also from problem solving perspective focuses on the effects of ionic potential on the properties of many materials. accurately grasp the connotation and extension of the concept, the ion potential and polarizability of the two important physical understanding of the deepening of the construction of the thinking model, broaden the application field of vision, the great benefit of chemical learning.

Keywords: ionic potential effective charge effective radius electron transition charge transfer polarization deformabilit.

Classification: FOR code: 039999

Language: English



London
Journals Press

LJP Copyright ID: 925644
Print ISSN: 2631-8490
Online ISSN: 2631-8504

London Journal of Research in Science: Natural and Formal

Volume 19 | Issue 2 | Compilation 1.0



© 2019. Wang Hai-Jun. This is a research/review paper, distributed under the terms of the Creative Commons Attribution-Noncommercial 4.0 Unported License <http://creativecommons.org/licenses/by-nc/4.0/>, permitting all noncommercial use, distribution, and reproduction in any medium, provided the original work is properly cited.

Ion Potential Principle Summary

Wang Hai-Jun

ABSTRACT

In this paper, in addition to the ionic potential of the meaning, influencing factors, variation, polarizability and the relationship of extensive and in-depth discussion, also from problem solving perspective focuses on the effects of ionic potential on the properties of many materials. accurately grasp the connotation and extension of the concept, the ion potential and polarizability of the two important physical understanding of the deepening of the construction of the thinking model, broaden the application field of vision, the great benefit of chemical learning.

Keywords: ionic potential effective charge effective radius electron transition charge transfer polarization deformability.

Author: The Beijing No 12 High School Chemical Innovation Experiment Center Beijing China).

I. INTRODUCTION

Ion potential is an important physical quantity used to measure the ability of ions or charged atoms to attract (or repel) electrons (clouds). It can qualitatively or semi-quantitatively explain some chemical facts and is widely used in the field of chemistry.

1.1 The meaning of ionic potential

1.1.1 Definition of G.H. Cartledge [1]

The ratio of ionic charge to ionic radius, i. e.

$$\varphi = Z/r$$

In the upper formula, Z is charged with ions and r is ionic radius (pm).

1.1.2 Definition of structural chemistry

$$\varphi = Z^*/r^*$$

In the formula above, Z^* is the effective charge [2] (net charge or formal charge) of an ion or atom, and r^* is the effective ion radius or the effective covalent radius of an atom. The effective charge Z^* can be determined by Slater approximation rule [2] according to the principle of drilling through effect and shielding effect. The meaning and numerical value of r^* can be found in reference [2]. These definitions are applicable to simple ions and charged atoms (such as B^{+3} , S^{+6} , Cl^{+7} , etc.), and can also be regarded as positive ions. They are more accurate, scientific, factual and widely used. For example:

$$S^{+6} : Z^* = +6, \quad r^* = 30pm, \quad \varphi(S^{+6}) = 0.200$$

$$Mn^{+7} : Z^* = +7, \quad r^* = 25pm, \quad \varphi(Mn^{+7}) = 0.280$$

$$S^{2-} : Z^* = -2, \quad r^* = 184pm, \quad \varphi(S^{2-}) = -0.019$$

The physical meaning of ion potential can be simply understood as: ion potential is a physical quantity used to measure the ability of an ion or charged atom to attract or repulse electrons (clouds).

1. $\varphi > 0$, Positive ion $\varphi > 0$, Negative ion $\varphi < 0$;
 $\varphi(\text{Positive ion}) \gg \varphi(\text{Negative ion})$;
2. Positive ions play an important role in attracting electrons (clouds). φ The greater the φ , the stronger the ability to attract electrons (clouds) ;
3. The negative ions are mainly repulsive to electrons (clouds). The smaller the φ , the stronger the ability to reject electrons (clouds).

II. MAIN FACTORS AFFECTING ION POTENTIAL OF POSITIVE IONS

2.1 Z^* Effective charge Z^* of ions

When r^* is close, the larger the Z^* , the larger the φ .

2.2 Effective radius of ions r^*

When Z^* is the same, the smaller the r^* , the larger the φ .

2.3 Electron layer structure of ions

The positive ions, which are similar to Z^* and r^* , are mainly determined by the valence electron structure of ions. The relationship between ionic potential and valence electron layer structure (configuration) is roughly:

$$\varphi(8e^-) < \varphi(9e^- - 17e^-) < \varphi(18e^-, (18+2)e^-)$$

For example, Zn^{2+} and Ag^+ are $18e^-$ positive ions with larger ionic potential. While Na^+ and K^+ are the positive ions of the $8e^-$ electron configuration, the ionic potential is smaller. This is mainly due to the fact that the valence electron layer of $9e^- - 17e^-$ or $18e^-$ or $(18+2)e^-$ positive ions contains d^x electrons, while that of $8e^-$ positive ions has no d electrons. Because d electron cloud has smaller penetration effect, weaker nuclear control, farther extension and smaller shielding effect on the nucleus, its effective nuclear charge Z^* increases with the increase of x , which leads to the increase of ion potential φ .

[Explanation] The factors affecting ion potential are complex and multi-factors cooperate; ion potential is dynamic and changeable, i.e. ion potential corresponds to the state of ion one by one; ion potential has clear physical meaning, but it has not been given dimension at present.

G. H. Cartledge's definition of ionic potential: $\varphi = Z/r$ is based on the ionic bond model, so it can only meet some facts. Some people also use ionic function such as $\varphi = Z/r^2$ or $\varphi = Z^2/r^3$ to express ionic potential to match some other facts. It should be said that the definition of $\varphi = Z^*/r^*$ is more reasonable. At present, ionic potential is still a developing concept.

III. LAWS OF IONIC POTENTIAL

3.1 The same period of periodic table of elements

From left to right: the positive ions distributed outside the core are reduced with the increase of Z^* , and r^* decreases. Such as:

$$\varphi(Al^{3+}) > \varphi(Mg^{2+}) > \varphi(Na^+), \varphi(Tl^{3+}) > \varphi(Hg^{2+}) > \varphi(Au^+)$$

3.2 The periodic table of elements is the same as the main group (elements s and p).

From top to bottom: positive ion: Z^* is the same, r^* increases, therefore, with the increase of atomic number, φ decreases; negative ion: $Z^* < 0$, Z^* is the same, r^* increases, therefore, with the increase of atomic number, φ increases.

[Explanation] When discussing the properties of the same period or group elements (e.g. metallicity), it is necessary to discuss them according to the actual size of the ion potential. At this time, Z^* and r^* determine the ion potential together.

3.3 Positive ions of different valence states of the same elements

The larger the Z^* , the smaller the r^* and the larger the φ . Such as:

$$\varphi(Cr^{6+}) > \varphi(Cr^{4+}) > \varphi(Cr^{3+}) > \varphi(Cr^{2+})$$

3.4 Rare earth element

Because of the shrinkage of lanthanide, the ion potential of rare earth elements is very close. Therefore, the properties of rare-earth elements are very close, coexistence and symbiosis, and separation is very difficult. Our country adopts Xu Guangxian's innovative grading extraction technology to separate the technology, leading the world.

3.5 The elements with similar ionic potentials are similar in nature.

Diagonal Similarity Principle: The adjacent elements (Li and Mg; Be and Al; B and Si, etc.) in the diagonal periodic table are similar in nature,

but far from other elements of the family. This is mainly due to the fact that the values of the ionic potentials of the two elements are similar, while the values of the ionic potentials of the other elements of the family are quite different.

3.6 The relationship between ionic potential and electronegativity

According to the definition of electronegativity by Allred-Rochow [2]:

$$X_{AR} = 3590Z^*/r^2 + 0.744 = 3590\phi/r + 0.744$$

It can be seen that the larger the ion potential, the larger the electronegativity X_{AR} , the positive correlation between the two, with essential consistency.

3.7 Relationship between ionic potential and ionic deformability

3.7.1 The meaning of ionic deformability

Under the electric field of other ions around the specified ion, the polarization deformation of the electron cloud around the ion occurs. Usually, the polarizability of the ion is described quantitatively by the ionic polarizability μ [3]. The larger the μ , the stronger the ion deformability.

3.7.2 Relationship between ionic potential and ionic polarizability

I. Positive ions: the larger the ionic potential, the smaller the polarizability is, for example:

$$\phi(\text{Fe}^{3+}) > \phi(\text{Fe}^{2+}), \mu(\text{Fe}^{3+}) < \mu(\text{Fe}^{2+})$$

$$\phi(\text{B}^{3+}) > \phi(\text{Al}^{3+}) > \phi(\text{Sc}^{3+}) > \phi(\text{Y}^{3+}) > \phi(\text{La}^{3+})$$

$$\mu(\text{B}^{3+}) < \mu(\text{Al}^{3+}) < \mu(\text{Sc}^{3+}) < \mu(\text{Y}^{3+}) < \mu(\text{La}^{3+})$$

II. Negative ions: Because of its $Z^* < 0$, therefore, the greater the ion potential, the greater the polarizability, such as:

$$\phi(\text{O}^{2-}) < \phi(\text{S}^{2-}) < \phi(\text{Se}^{2-}) < \phi(\text{Te}^{2-})$$

$$\mu(\text{O}^{2-}) < \mu(\text{S}^{2-}) < \mu(\text{Se}^{2-}) < \mu(\text{Te}^{2-})$$

III. The difference between Z^* and r^* is different. The larger the r^* , the greater the polarizability.

$$r^*(\text{I}^-) > r^*(\text{Br}^-) > r^*(\text{S}^{2-}) > r^*(\text{Cl}^-) > r^*(\text{O}^{2-}) > r^*(\text{F}^-) [3]$$

$$\mu(\text{I}^-) > \mu(\text{Br}^-) > \mu(\text{S}^{2-}) > \mu(\text{Cl}^-) > \mu(\text{O}^{2-}) > \mu(\text{F}^-) [3]$$

IV. Positive ions with d^x electrons: Because of the large deformability of d orbital, the deformability of positive ions with d^x electrons is generally strong. For example, Ag^+ has larger ϕ and μ .

[Conclusion]] Positive ions: The larger the ion potential is, the stronger the polarization ability is, and the weaker the deformability is, that is, the smaller the polarizability is. Negative ions: The bigger the ion potential is, the bigger the polarizability is, the bigger the deformability of the ion itself is. The ionic potential generally corresponds to the polarization ability of ions, and the rate of polarizability generally corresponds to the deformability of ions.

[Note] I^- , Br^- , S^{2-} are strongly deformable negative ions, while O^{2-} , F^- are weakly deformable negative ions; Ag^+ , Zn^{2+} , Cd^{2+} , Hg^{2+} are strongly deformable positive ions, while Li^+ , Na^+ , Be^{2+} , B^{3+} are weakly deformable positive ions.

3.7.3 The matching principle between the ionic potential and the polarizability

1. The larger the ion potential is, the larger the polarizability is. The polarization deformation of the negative ion is mainly caused by the positive ion. For example, $\phi(\text{Fe}^{3+}) > \phi(\text{Fe}^{2+})$, $\mu(\text{I}^-) > \mu(\text{S}^{2-})$, both FeI_2 and FeS can exist stably; Fe_2S_3 exists, but its stability is poor; FeI_3 does not exist. How to explain? The answer is in this article!
2. The interactions between the two ions with large ionic potentials (or small polarizabilities) are relatively small.
3. There is a strong interaction between positive ions with larger ionic potential and polarizability (the valence layer contains d^x electrons) and negative ions with larger polarizability.

[Explanation] Experience shows that the ionic potential is determined by Z^* and r^* together, while the polarizability is mainly determined by r^* [3]; the ionic potential is generally used to describe positive ions, and the polarizability is generally used to describe negative ions. Therefore, it can be said that the surface of ionic potential and polarizability are opposite and essentially unified, "i.e., enemies and narrow paths"; the two models are different, the angles of dealing with the problem are different, the paths are the same, and can not be neglected.

IV. SIMPLE APPLICATION OF IONIC POTENTIAL

4.1 Influence of ionic potential on the type of chemical bond

The enhanced polarization between positive and negative ions bound by chemical bonds can lead to changes in the types of chemical bonds.

Generally speaking, when positive ions with large polarization ability (big φ) and strong deformability (big μ) are combined with negative ions with strong deformability (big μ), the distribution of charges (electronic clouds) of each other is greatly changed by strengthening the interaction of polarization, thus shortening the distance between ions, leading to orbital overlap (overlap, reorganization), and chemical bonds. The ionic component decreases while the covalent component of the chemical bond increases. The transition from the ionic bond to the covalent bond leads to the transformation of the chemical bond type and even the corresponding crystal type, which causes the change of some properties of the substance.

Particularly noteworthy is that positive ions (such as Ag^+ , Zn^{2+} , Cd^{2+} , Hg^{2+}) with strong polarization ability and deformability of the electronic layer structure containing d^{10} and negative ions (such as I^- , S^{2-} and so on) with strong deformability will deform the electron cloud around the ion due to the polarization interaction (additional polarization). Both the type of chemical bond and the corresponding crystal type are transformed.

For AgCl , if the distance $d(d=r_+ + r_-)$ is calculated according to the ionic bond model, it should be 294 pm , whereas the actual measurement is 287 pm . Obviously, due to the interaction of polarization, the distance between nuclei is shortened by 17 pm , the covalent bond composition in AgCl increases significantly, and AgCl crystals become "mixed or transitional crystals" rather than pure ionic crystals. Based on the stronger interaction of polarization, the distance between nuclei of AgI is even shortened by 52 pm , so that the chemical bonds in AgI are mainly covalent bonds, and AgI crystals become ZnS-type molecular crystals rather than NaCl-type ionic crystals.

Another example is that Li^+ has a small radius ($r_{\text{Li}^+}=68\text{pm}$, $r_{\text{Na}^+}=98\text{pm}$) and a large ionic potential. Therefore, Li^+ has a strong polarization ability in alkali metals, and has the greatest tendency to form covalent bonds. It can form covalent compounds, while other alkali metals basically form ionic compounds. Based on this, compared with other alkali metal ions of the same family, Li^+ exhibits many different special properties, for example, LiOH is moderately strong alkali. This is mainly due to the obvious covalence of Li-O bond due to the polarization of Li^+ and the change of the dissociation mode of LiOH (partially acid dissociation). Other alkali metal hydroxides (MOH) are strongly alkaline, mainly ionic compounds.

The radius of Be^{2+} ion in the main group of IIA is smaller than that of Li^+ and the charge is twice that of Li^+ so that the charge density of Be^{2+} is higher, the ionic potential is larger and the polarization ability is stronger. It can even cause polarization deformation of F^- and O^{2-} with very low polarizability, which results in the covalent bonding of Be with almost all other elements. There is no simple ion of Be^{2+} in the solution, only in the form of hydrated ion $\text{Be}(\text{H}_2\text{O})_4^{2+}$ in strong acidic solution (strong polarization of O in water molecule), and even the Be-F bond in BeF_2 formed by the most electronegative fluorine element has obvious covalence. BeF_2 molecule is a few metals that can not be completely ionized in solution. One of fluoride.

The valence electron configuration of boron (B) atoms in the main group of III A in the periodic table of elements is $2s^2 2p^1$, the radius of boron atom is small (85-90pm), and the ionization energy is high ($I_1=8.296\text{eV}$, I_2 and I_3 are much larger than I_1). This shows that the effective nuclear charge Z^* of B^{3+} is large, the attraction of valence layer electrons is great, the ionic potential is large, and boron is almost all bound by covalent bonds with other elements. On the other hand, the polarization ability of B^{3+} ions is very strong. In the solution, there is no simple ion of B^{3+} , but it acts with H_2O molecule to form $B(OH)_3$.

4.2 Influence of ionic potential on solubility of compounds

The solubility of compounds is related to many factors, and the dissolution process is a very complex physical and chemical process. Various theories, hypotheses and models [4] 550 are still immature, and most of them are only approximate and empirical laws. For example, the principle of similarity and compatibility, which is an empirical rule summarized from a large number of experimental facts, can explain some facts. According to this principle, ionic compounds and strong polar covalent compounds are easy to dissolve in polar solvents (such as H_2O (l), NH_3 (l), etc.), while non-polar or weak polar covalent compounds are easy to dissolve in non-polar solvents (such as benzene, carbon tetrachloride, etc.). Strictly speaking, compounds with similar dipole moment are easy to dissolve each other.

Because of the polarization between ions, the chemical bond type in some compounds transits from ionic bond to covalent bond, resulting in the decrease of dipole moment and polarity of the compounds, and the corresponding decrease of solubility of the compounds in strong polar solvent water. For example, the radius of Ag^+ is between Na^+ and K^+ ($r_{Ag^+}=126\text{pm}$, $r_{Na^+}=95\text{pm}$, $r_{K^+}=133\text{pm}$), but the solubility of $AgCl(s)$, $NaCl(s)$, $KCl(s)$ is quite different. The change of Gibbs free

energy ($\Delta_{\text{sol}}G$), which indicates the spontaneous dissolution trend, is respectively: $+55.6\text{kJ}\cdot\text{mol}^{-1}$, $-92\text{kJ}\cdot\text{mol}^{-1}$, $-6.7\text{kJ}\cdot\text{mol}^{-1}$, so it can be inferred that their solubilities are quite different. The same is true: $AgCl(s)$ is insoluble in water ($p^{K_{sp}(AgCl)}=9.75$), $NaCl(s)$ and $KCl(s)$ are soluble in water. The solubility of $AgCl(s)$ is obviously related to the valence electron structure of Ag^+ . On the one hand, because the valence electron configuration of Ag^+ is $4d^{10}5s^0(9e^- -17e^-$ configuration, while Na^+ and K^+ are $8e^-$ configuration), the effective nuclear charge Z^* of Ag^+ is larger and the ionic potential is larger; on the other hand, the polarizability of Ag^+ is much larger because the D electron cloud is easily polarized and deformed. It is also larger. In this way, the Ag-Cl bond is strengthened due to the interaction of polarization, the ionic component of the bond decreases while the covalent component increases, resulting in the decrease of dipole moment and the decrease of solubility in polar solvent water. It can be expected that the solubility of $NaCl(s)$ and $KCl(s)$ is also quite different (why? Please seek an explanation in this article).

Compared with silver halide $AgX:AgF(s)$, the F ion potential of fluoride ion in $AgX:AgF(s)$ is smaller, the polarizability is smaller and the deformability is weaker, so the interaction between Ag^+ and F is very small. The ionic composition of Ag-F chemical bond is larger. $AgF(s)$ is still an ionic crystal, and the dipole moment of AgF is larger, so it is soluble in polar solvent water. For $AgCl$, $AgBr$ and AgI , due to the strong mutual polarization between Ag^+ and X ions, the covalent component of Ag-X chemical bond is increased, the dipole moment of AgX is reduced and the polarity is weakened, so that they are insoluble in water ($p^{K_{sp}}(AgBr)=12.3$, $p^{K_{sp}}(AgI)=16.08$), and with the mutual polarization between Ag^+ and X gradually. The solubility of $AgCl(s)$ to $AgBr(s)$ to $AgI(s)$ decreases gradually.

The solubility of $Li_3PO_4(s)$ and $Li_2CO_3(s)$ in water is much lower than that of salts corresponding to other alkali metals in the periodic table of elements.

4.3 Influence of ionic potential on the color of compounds

Basic Principle of Matter's Color Presentation: The interaction between light and matter causes the transition of electrons in matter between different energy levels, leading to the selective absorption and emission of light by matter. The physical processes of reflection, transmission, deflection and scattering can occur when light of different wavelengths is transmitted in matter. Human's perception of material color is based on the comprehensive effect of the above process on human's visual perception. All of these are related to material structure.

In addition to changing the type of chemical bond, positive ions with high ionic potential can also change colorless ions into colored ones. These changes are related to the internal structure of molecules or ions that constitute substances. In the formation of compounds, the polarization of the electron cloud of the ligand (atom, molecule or ion which distributes around the positive ion and binds directly with it) can be deformed, so that the energy levels of the electrons in the system can be recombined, and the energy level difference $\Delta E = h\nu$ (ν where ν is the frequency of light, the same below) can be changed. The change results in the change of the frequency and wavelength λ of the absorbed light and the change of the frequency and wavelength λ of the emitted light when the electron undergoes the energy level transition, so that the original colorless ions become colored after the formation of compounds.

Typical ionic compounds generally do not absorb light in the visible region of the spectrum, so they appear colorless or white under visible light (white light), for example, KCl is a colorless solid. The basic principle is that in typical ionic compounds, if it takes a great deal of energy to make electrons transit from negative ions to positive ions, the ultraviolet light of high frequency and short wave should be absorbed from $\Delta E = h\nu$ and $\lambda = c/\nu$ (c is the speed of light). When a typical ionic compound absorbs light

from the ultraviolet region, it generates charge transfer (charge transfer transition, see below) absorption spectra. However, when the light of the ultraviolet region is absorbed, the band is colorless, that is, the substance is colorless.

By strengthening the polarization of the ligand, the central ions with high ionic potential promote the electron cloud to migrate gradually from the ligand to the central ion, which decreases the density of the electron cloud around the ligand and increases the energy level of the atomic orbital or molecular orbital, which leads to the increase of the energy of the electrons in the original ground state of the ligand. The energy level difference between the highest occupied orbital level of the ligand and the lowest empty orbital of the central ion decreases, and the transition (transfer) of electrons between the ligand and the central ion becomes easier. From $\Delta E = h\nu$ and $\lambda = c/\nu$, we know that the absorbed light will move in the direction of low frequency and long wave. Therefore, only absorbing a certain wavelength of light in the visible region can cause the excited state electrons in the highest occupied orbit of the ligand to transit to the low energy space orbit adjacent to the central ion, thus showing the color in the visible region, which is called color rendering.

The transition of electrons between central ions and ligands is usually called charge transfer transition, which corresponds to the electron transfer occurring inside the system and is a form of electron transition.

The necessary condition for charge transfer transition is that the energy of the lowest empty orbit of the ligand is higher than that of the lowest empty orbit of the central ion, so as to ensure that the excited state electrons in the highest occupied orbit of the ligand can transit to the lowest empty orbit of the central ion more easily without transiting to the ligand itself. The lowest orbit on the body. This self consistent condition can be satisfied by polarization.

The wavelength range of the light absorbed by the charge-transfer transition depends on the energy difference between the lowest space orbit of the central ion and the highest occupied orbit energy level of the ligand. Thus, it is not difficult to understand: (1) For compounds with the same central ion but different ligands, the more deformable the ligand (the greater the polarizability μ) is, the less energy is needed for the charge transfer transition, and the more color the material presents moves to the direction of long wave, i.e. the color deepens. For example, the color of AgCl to AgBr to AgI gradually deepens. (2) For compounds with the same ligand but different central ions, if the central ions belong to the isomorphous ions, the energy required for charge transfer transition generally decreases with the increase of the ion potential of the central ions, and the color of the substance gradually moves towards the long wave direction, that is, the color gradually deepens. For example, $ZnI_{2(s)}$ is colorless, $CdI_{2(s)}$ is yellow, $HgI_{2(s)}$ is red, and color gradually deepens.

Some covalent halides or sulphides with d^{10} electronic structure of central ions show darker colors. For example, AgBr is yellowish, AgI, CdS, PbI_2 are yellowish, HgS is red and so on. The color deepens gradually, indicating that the charge transfer transition becomes easier. The main reasons for the above changes are as follows: ionic potential $\varphi (Hg^{2+}) > \varphi (Pb^{2+}) > \varphi (Cd^{2+}) > \varphi (Ag^+)$, and the polarizability of I and S^{2-} are larger, and the interaction between positive and negative ions is stronger. In addition, the central metal ions in these compounds have d^{10} electronic structure, and the d electron layer is full, that is, the low-level orbits are full. In order to have their own electronic transitions (i.e., $d-d$ transitions), it is necessary to jump to the higher-level orbits. The energy required is much larger than that of visible light. If the electron of the ligand moves to its own high-level orbit, it also needs higher energy, but the charge transfer transition between the ligand and the central ion requires less energy, which can be achieved by absorbing some wavelength of light in the visible region. Apparently, the

Colouring Mechanism of these compounds is the result of charge transfer transition, i.e. electron transfer in the system caused by strong polarization between ligand and central ion, which is the evidence of charge transfer transition.

It should be pointed out that the ionic potential can only affect the color of the compound, but it can not determine the color of the compound (the intensity of the color). The color of the compound depends on the probability of electron transition. The greater the probability of transition (allowing transition), the darker the color; the smaller the probability of transition (forbidden transition), the lighter the color. Ion potential only affects the wavelength and frequency of the light absorbed during the transition. If the light absorbed in the ultraviolet or infrared region is colorless. Therefore, the larger the ionic potential is, the more complex the color of the compound is.

4.4 Influence of ionic potential on acid-base ionization

Oxyacids and bases are essentially isomorphous substances, that is, they are compounds containing hydroxyl groups (OH). It can be simply expressed by **R-O-H**. According to structural analysis, R-O-H may have two ways of breaking chemical bonds: 1. breaking R-O bond; 2. breaking O-H bond. If the R-O bond is broken mainly by alkali ionization, if the O-H bond is broken mainly by acid ionization, if the two bond breaking abilities are equal, it is "amphoteric" ionization. The way of ionization depends on the polarization of the central ion (atom) and the polarity induction effect of the water molecule. In the final analysis, it is equivalent to the "contest" for the central O atom of R-O-H. A model of action is proposed here: $H_2O \cdots R-O-H \cdots OH_2$, H-O-H molecules at both ends (R-end and H-end) induce electron clouds in the system in opposite directions and with different intensities. If the value of the ionic potential of the central ion is larger, the polarization effect is stronger, and the power of R^{+n} attracting oxygen atom electron cloud is greater. Through the interaction of R^{+n}

polarization and the polarity induction effect of the left-end hydrogen peroxide, the density of oxygen atom O electron cloud is reduced, the R-O bond is shortened, the O-H bond is lengthened, and the bond force of O-H bond is weakened. The O-H bond is covalent bond. The trend of conversion to ion bond increases, the polarity of O-H increases, and the dipole moment of the bond increases, then acid ionization occurs mainly by breaking the O-H bond, resulting in H^+ . On the contrary, if the value of the ionic potential of the central ion is smaller, the polarity induction of the right-end hydrogen oxide molecule will be greater than that of the central ion (atom) R^{+n} and the left-end hydrogen oxide molecule pole. The sum of sexual induction makes the R-O bond lengthen and weakens the bonding force of the R-O bond. The weaker the covalent component of the R-O bond, the larger the ionic component of the bond, the greater the polarity of the R-O bond and the increase of the bond dipole moment, the basic ionization of the R-O bond mainly breaks and produces OH^- . The acidity and alkalinity of ROH are mainly determined by the synergistic effect of the ion potential of R^{+n} and the polarity induction effect of water molecule. A semi-quantitative relationship between acid and alkali of ROH-type compounds related to the ionic potential of R^{+n} has been proposed.

1. $\varphi < 0.048$, ROH The main manifestation is basic ionization.
2. $0.048 < \varphi < 0.102$, ROH Two types of ionization coexist, that is, acid type and basic ionization.
3. $\varphi > 0.102$, ROH Acid ionization is the main feature.

When the electronic layer structure of the central atom R^{+n} of ROH is the same, the greater the ionic potential of the central ion (atom), the stronger the acidity, the smaller the ionic potential, and the stronger the alkalinity. For example, in NaOH, $\varphi(Na^+) = 0.001 < 0.048$, NaOH mainly occurs alkaline ionization, showing strong alkalinity; in $Al(OH)_3$, $0.048 < \varphi(Al^{3+}) = 0.059 < 0.102$, $Al(OH)_3$ occurs two kinds of properties of ionization coexist, and alkaline ionization is stronger than

acidic ionization, showing very weak alkalinity; in H_2SO_4 , $\varphi(S^{6+}) = 0.200 > 0.102$, H_2SO_4 mainly occurs acidic ionization, showing strong alkalinity. Strong acid.

[question] by contrast, why is "gender" ionization very weak? Please seek an explanation from this article.

4.5 Effect of Ion Potential on Other Properties of Compounds

4.5.1 Effect of Ion Potential on the Reaction Performance of Salts with Water

When salts dissolve in water, the positive and negative ions released by salts hydrate with water molecules and coordinate with a certain number of water molecules around the positive and negative ions, which are then strengthened by ion polarization. If the ion potential of metal positive ions is large and the polarization ability is strong, the bond force of O-H chemical bond in water molecules can be greatly weakened by polarization. At the same time, under the constant collision of water molecules or other particles in water, some additional energy can be obtained. At this time, the O-H bond in more water molecules may break, resulting in OH^- and H^+ . Then the positive ions of salt can capture OH^- and then OH^- can be obtained. If the H^+ released by water itself can polarize the negative ions of salt and penetrate into the electron cloud of the negative ions, it will combine with the negative ions directly, which is equivalent to the catching of H^+ by the negative ions and releasing OH^- , the above two processes can also be carried out simultaneously. As a result, the ionization equilibrium of water is destroyed, resulting in the continuous ionization of OH^- and H^+ . When the equilibrium is re-established, the relative concentration of OH^- and H^+ ($c(H^+)/c(OH^-)$) in the solution changes, making the solution acidic or alkaline, which is the essence of saline hydrolysis. [Conclusion] The hydrolysis reaction of anion is complex, and its hydrolysis ability is inversely proportional to the acid strength of its conjugated acid (K_{θ}). The weaker the conjugated acid is, the stronger the hydrolysis reaction of its acid

radical anion (i.e. its conjugated base), such as CO_3^{2-} , SiO_3^{2-} , etc. The higher the ion potential of positive ions, the stronger the hydrolysis reaction ability.

4.5.2 Effect of Ion Potential on Crystal Lattice Type

Because of the strong polarization, the type of chemical bond changes from ion bond to covalent bond. This transition not only shortens the distance between ions, but also tends to reduce the coordination number of crystals, leading to the change of crystal type. For example, according to the ionic bond model, the radius ratio of positive and negative ions of CdS is calculated to be $r(+)/r(-)=0.53$. Therefore, CdS should belong to NaCl-type crystal with coordination number 6, whereas CdS belongs to ZnS-type crystal with coordination number 4. The reason is that Cd^{2+} has larger ionic potential and stronger polarization ability, while S^{2-} has strong deformability. Cd^{2+} can partially penetrate into the electronic cloud of S^{2-} as if it reduced the ionic radius of Cd^{2+} to 0.44 instead of 0.53, thus changing the lattice type.

4.5.3 Effect of Ion Potential on Conductivity and Metallicity of Compounds

Because of the polarization, the electrons in negative ions tend to be separated from the negative ions, and the fluidity of these electrons is enhanced, which is equivalent to the free electrons in metals. Thus, the lattice of the crystal can be transformed from the lattice of the ionic crystal to the lattice of the metallic crystal, and the conductivity increases, and the metallicity increases accordingly. The opacity and metallic luster of sulfides are related to this, such as FeS, CoS, NiS and other chemical powders, especially their ores, all have metallic luster.

4.5.4 Effect of Ion Potential on Thermal Stability of Compounds

The polarization of ions with high ionic potential is stronger. Because of the polarization of positive ions in the compound, the thermal stability of the

compound is weakened and the decomposition reaction is easy to take place. For example: $\varphi(\text{Li}^+) > \varphi(\text{Cu}^{2+}) > \varphi(\text{Ag}^+) > \varphi(\text{Na}^+)$, LiOH red heat is decomposition, $\text{Cu}(\text{OH})_2$ heating decomposition, NaOH does not decompose; AgNO_3 heating decomposition, NaNO_3 strong thermal decomposition.

4.5.5 Effect of Ion Potential on Thermal Stability of Metal Hydride

In alkali metal and alkaline earth metal binary hydrides, because H has a larger radius (208pm), it is easy to deform and polarize, so when it is combined with positive ions with larger ion potential, the type of chemical bond will transit from ion bond to covalent bond, and the strength of chemical bond will also increase, thus enhancing its stability. For example: LiH heating does not decompose, while NaH heating is easy to decompose into metal sodium and hydrogen, because: $\varphi(\text{Li}^+) > \varphi(\text{Na}^+)$, Li^+ polarizes more strongly than Na^+ and LiH is more stable than NaH.

4.5.6 Influence of ionic potential on other properties of compounds

Many elements, especially transition metal elements, often show different oxidation states in different compounds, and the existence of various stable oxidation states is closely related to ion potential. Ions with high ionic potential generally can not form simple ions, they all exist in the form of complex ions; ions with low ionic potential can generally form simple ions. For example, Mn^{2+} ion can exist stably in aqueous solution, while Mn^{+7} ion can only exist in the form of MnO_4^- in aqueous solution; S^{+6} ion can not exist in the form of S^{6+} simple ion, but only in the form of SO_4^{2-} hydrated ion.

[Summary] Thinking model: ionic potential, deformability → polarization, mutual polarization → polarity change of bond → transition from ionic bond to covalent bond (bond type change, crystal type change) → variety of properties change.

It should be pointed out that at present the ion potential can only explain qualitatively or semi-quantitatively some properties of elements or compounds, and the properties of elements or compounds are often the synergistic representation of many factors. For example, the strength of oxyacid depends not only on the ionic potential of the central ion, but also on the number of non-hydroxyl oxygen atoms around the central ion and other factors ^[1]⁹⁴; the solubility of ionic compounds is also related to their lattice energy, and so on. Therefore, when using ion potential to explain the problem, we should pay attention to its scope of application and role, and consider the problem comprehensively.

In this paper, the principle and application of ionic potential are simply summarized and sorted out, focusing on throwing bricks and attracting jade. The shortcomings are unavoidable, such as inadequate structural analysis, no thermodynamic analysis and so on. Thank you for your comments and comments.

REFERENCE

1. Li Mingxiu, Li Binghuan. Selections of inorganic chemistry. Beijing: Beijing Institute of Technology press, 2004:94-94
2. Zhou Gonggong, Duan Lianyun. Basis of Structural Chemistry. 2 Edition. Beijing: Peking University Press, 2002: 432- 434. 65-65.81-81
3. Xu Guangxian, Wang Xiangyun. Material structure. 2 edition. Beijing: Science Press, 2013:661-661
4. Fu Xiancai, Shen Wenxia, Yao Tianyang. Physical Chemistry. 4 Edition. Beijing: Higher Education Press, 2001:550-550.



Scan to know paper details and
author's profile

Consortium Building among Academic Libraries in Nigeria: The Legal and Ethical Considerations

Abiola, A. Abioye & Olalekan Abiola Awujoola

University of Ibadan

ABSTRACT

The ever increasing and complex needs of information users, accelerated rate of information explosion, dwindling library budget, escalation of prices of information resources and many more have given rise to a set of pressing problems in providing adequate and relevant services by academic libraries and information centres across the globe. As a solution to these problems, taking advantages of Information and Communication Technology (ICT), libraries have started sharing their resources and services through consortium to satisfy their users better. The multi-disciplinary and multi-dimensional nature of the library and information science profession in the 21st century has created opportunities and challenges for information centres in developing countries like Nigeria which wise to join consortium platforms. It is imperative then that libraries consider legal and ethical requirements to consortium building as a way of ensuring sustainable collaboration platforms among them. This study examines some legal and ethical factors necessary for consortium building in Nigeria.

Keywords: consortium building, academic libraries, legal factors to consortium, ethical factors to consortium.

Classification: FOR code: 080799

Language: English



London
Journals Press

LJP Copyright ID: 925645
Print ISSN: 2631-8490
Online ISSN: 2631-8504

London Journal of Research in Science: Natural and Formal

Volume 19 | Issue 2 | Compilation 1.0



Consortium Building among Academic Libraries: The Legal and Ethical Considerations

Abiola, A, Abioye ^α & Olalekan Abiola Awujoola ^σ

ABSTRACT

The ever increasing and complex needs of information users, accelerated rate of information explosion, dwindling library budget, escalation of prices of information resources and many more have given rise to a set of pressing problems in providing adequate and relevant services by academic libraries and information centres across the globe. As a solution to these problems, taking advantages of Information and Communication Technology (ICT), libraries have started sharing their resources and services through consortium to satisfy their users better. The multi-disciplinary and multi-dimensional nature of the library and information science profession in the 21st century has created opportunities and challenges for information centres in developing countries like Nigeria which wise to join consortium platforms. It is imperative then that libraries consider legal and ethical requirements to consortium building as a way of ensuring sustainable collaboration platforms among them. This study examines some legal and ethical factors necessary for consortium building in Nigeria.

Keywords: consortium building, academic libraries, legal factors to consortium, ethical factors to consortium.

Author α: Department of Library, Archival and Information Studies, University of Ibadan.

σ: Department of Library, Archival and Information Studies, University of Ibadan.

I. INTRODUCTION

The advent of Information and Communication Technology (ICT) has made information to grow exponentially, however, it has also created great possibility for libraries to come together to share their resources (electronic library resources) through a network called “Consortium”. Consortium platforms provide opportunity for wider and more coordinated resource sharing among cooperating libraries or institutions. A library consortium in library world is defined as a cooperative arrangement among libraries, with non-profit making intention, seeking to create and maintain a shared online catalogue and provide user services for both members and non-members (American Heritage Dictionary, 2017). Resource sharing has become a very effective and useful tool in consortium building, since no one library can afford to acquire all resources, even, if it is in its own special areas (Sacchanand, 2012). A consortium can also be said to be the ultimate collective approach in reaching information goals and meeting information needs of users through shared electronic library resources and reciprocal borrowing, offsite storage system, and other cooperation and services to members and non-member libraries. Ali, Owoeye and Anasi (2010); Etim (2006) opined that the terms “library cooperation”, “library networking”, “library linkages”, “library collaboration”, “library consortia”, “interlibrary loan”, “document supply”, “document delivery”, “access services”, “resources sharing” are used interchangeably to describe formal and informal cooperation, partnership and resource sharing activities among libraries.

The exponential growth of published materials both in a chosen field and other fields, coupled with the growth of published information scattered and presented in various electronic formats have made it impossible for any single library most especially university libraries to keep up in their quest to satisfy their user's information needs (Ukwoma, 2017). Therefore, cooperation or collaboration is inevitable among university libraries to facilitate information and resource sharing among them. Collaborations according to Mohammed (2015) can enhance the library's ability to serve its community and make library services more visible and valued. University libraries have a laudable history of cooperating to achieve common goals.

The need for consortium building among university libraries includes: increasing the cost benefit per subscription among cooperating libraries; promoting the rational use of funds in libraries; ensuring the continuous subscription to the periodicals subscribed to in each library; ensuring local storage of the information acquired by libraries for continuous use by present and future users; helping to develop technical capabilities of the staff in operating and using electronic publication databases; strategic alliance with institutions that have common interest; reduced information cost and improved resource sharing. Other reasons for the creation of consortium are to: eliminate the different problems faced by libraries in providing various services to users; meet the thrust of information of the vast people due to rapid growth of population all over the world (Murthy, 2002 and CALIBER, 2003, Hulagabali, 2012, Ukwoma, 2017).

II. LITERATURE REVIEW

Any consortium platform is a professional and business like arrangement intended for a defined purpose over a fixed timeframe. It is imperative, therefore, that the process and activities of the consortium should be approached in a business-like way. This is essential to protect the long term integrity of individual library and the

platform. This approach recognises both the benefits and hazards of "association". It recognises that whilst there are benefits which arise from association with strong and successful organisations, the converse is true where consortium members get into trouble and this reflects on other organisations in the consortium (CabinetOffice: Office of the Third sector. 2008). A major concern for libraries considering entering into consortium arrangements is that of sharing information and its services. There is a tension around a library providing sufficient information for the other members to be able to make a business judgment about their inclusion in their arrangements and the library wishing to withdraw from the consortium at a later stage. Securing compensation for a breach in legal terms in the consortium agreement can be costly and time consuming. It is essential therefore, that a legally binding agreement for the governing law, sharing of information, nondisclosure of log-in-option, dispute resolution, cash payment and contribution as well as terms of dissolution be documented. All potential consortium members should be invited to sign up to this agreement before any serious actions regarding the implementation of the consortium. In certain circumstances, the law will require the consortium members to keep matters confidential without a written agreement in place, but this can be difficult and costly to prove in court. It is always best when disclosing any kind of confidential information (particularly sensitive technical information) to have a "written confidentiality agreement" "legal" in place and signed by potential consortium members.

Business Dictionary.Com (2010) defines law as the binding rules of conduct meant to enforce justice and prescribe duty or obligation, and it is derived largely from custom or formal enactment by a ruler or legislature. Laws are rules that mandate or prohibit certain behaviour; they are drawn from ethics, which define socially acceptable behaviours. The cogent difference between laws and ethics is that laws carry the authority of a governing body (enforcement

agency), and ethics do not. Law derives its legitimacy ultimately from universally accepted principles such as the essential justness of the rules, or the sovereign power of a parliament to enact them. Law can also be viewed as a system of rules which a particular country or community recognizes as regulating the actions of its members and how it may be enforced by imposing penalty or fine (Ogunleke, 2015). Ethics differs as it provides basic social needs by defining the behaviour we expect and will accept from one another. Jean-Jacques Rousseau (2007) in his “Social Contract or Principles of Political Right” explains law as the rules the members of a society create to balance the individual rights to self-determination against the needs of the society as a whole. Ethics are based on cultural mores: the fixed moral attitudes or customs of a particular group. These rules describe the way in which people (libraries) are required to act in their relationship with others (libraries) in a society (platform) most especially a consortium (Ogunleke, 2015). Apart from the laws that individual country has, organisations and professional associations may as well provide a set of right and wrong that signals its members’ competencies and integrity thus providing social legitimisation to its members (Ike-Mbofoung, 2015). The United Nations (UN) Human Rights, International Federation of Library Associations (IFLA) and Institutions, and the Nigerian Library Association (NLA) monitor any legislation affecting library and information science profession; guide the management of members and their relationship with clientele. Aside the legal issues to be agreed on by member library, there is an acceptable way of relationship (ethical standards) required of members within the consortium.

Ethics is a very wide term that can be used in a variety of contexts. According to Anand (2008), ethics applies to any system or theory of moral values or principles. There can be company ethics, social ethics, business ethics, company ethics, professional ethics, family ethics and many more. Ethics is a word derived from the Greek word

“ethos” which implies customs and habit. Adekilekun (2008) says ethics is something in conformity with moral norms or standard of professional standards. Ethics becomes a principle in politics and social law (Ogunleke, 2015). According to Kumar (2007), ethics is concerned with the code of values and principles that enables a person to choose between right and wrong, and therefore, select from alternative course of actions. Erondu, Sharland and Okpara (2004) hold that the study of “ethics” focuses on issues of practical decision making, including the nature of ultimate value, and standards by which a human action can be judged right or wrong, good or bad. The study will view ethics in two-folds: Business ethics (libraries coming together for the business of satisfying their clientele the more) and professional ethics (libraries carry out professional activities). Therefore, libraries intending to join a consortium should observe both professional and business codes of conduct.

Jelena (2007) while trying to examine business ethics opined that business ethics (collective or business) is the effect of the social nature of morality, and the feedback effect of business morality on business environment. According to Haslinda and Benedict (2009), business ethics is a study of business activities, decisions and situations where the rights and wrongs are addressed. It is a form of applied ethics that studies rules and principles within a commercial context and any obligations that apply to persons who are involved in commerce. Ahmed (2013) says that business ethics is a form of applied ethics that examines rules and principles within a commercial context; the various moral or ethical problems that can arise in a business setting; and any special duties or obligations that apply to persons who are engaged in commerce. Nelson and Westerberg (2010) hold that ethics and business must go together, because doing business without observing some ethics is the surest way to fail. Bowie (2001) and Egels-Zanden and Sandberg (2010) also attest to the necessity of ethics in business communities and practices.

According to them, business ethics is about how the nature of business is understood as a morally compelling domain of human activity. Given that business activities (cooperation in librarianship) play a role in the society, it is expected that players in the cooperation behave as expected of them. The library as an organisation is in the business of providing information to the society, not necessarily to make profit but to incur enough returns to keep its business of information provision running. A library agrees and comes into consortium with other member libraries to provide better information services, this makes the library an entity in the cooperation formed.

Professional ethics on the other hand are the moral standards, principles, and regulation that guide the course of professional behaviour (Ali, 2013). Professional ethics are both individual and institutional in nature. Professional ethics can be learnt during the process of studying of the profession. Idolohor (2010) says professional ethics rely upon one's own personal sense of moral behaviour and judgment. The Association of Accountant Technicians (2011) defines professional ethics as personal and corporate standards of behaviour expected of the members of a particular profession. They are the ethical principles that a group or body of professionals must adhere to in the course of their interaction or business dealings in their professional life. An individual's behaviour can be unethical without it being illegal, therefore business or professional ethics cover wider area and scope than the law. Many professions that are trusted by the public are expected by the public to have code of ethics that guides their dealings and transactions. These codes spelt out the expectations of the behaviours of and the boundaries within which members have to operate (Ogunleke, 2015).

2.1 Legal considerations on consortium building

Governing laws: Nwalo and Ogunniyi (2012) asserted that for greater effectiveness, libraries embarking on networking should have a formal agreement (policy) in order to have workable

guidelines directing their operation. Collaboration among libraries should have a guiding principle as not much can be achieved under a loose arrangement.

Access and Log-in-options: Access to resources is now considered more important than the collection building. Consortium helps the collaborating libraries to get the benefit of wider access to electronic resources at affordable cost and at the best terms of licenses. A consortium, with the collective strength of resources of various institutions available to it, is in a better position to resolve the problems of managing, organising and archiving the electronic resources (Bedi and Sharma, 2008). However, the issues of access and log-in-option of members and affiliated bodies must be well considered in the consortium agreement. Access is decided on background and foreground contents of the consortium, consortium partners usually do not start their projects from scratch. They join the consortium with their own knowledge, data, etc., that are protected or not by the intellectual property right (IPR). In the terminology of the consortium projects this input is called "background". In addition, the project itself will generate new knowledge, data, etc. In the terminology of the consortium projects this output is called "foreground" (Foreground includes the tangible (prototypes, microorganisms, source code, etc.) and intangible (intellectual work, valuable business information, skills, abilities and scientific or industrial methods or applications processes developed) project results. Results generated outside a project (sometimes described as "Sideground") are not numbered among foreground) (Ambient Assisted Living (AAL), 2006).

Non-disclosure of log-in-option: Non-disclosure relates to issues of confidentiality among consortium members. Participants should know what knowledge they each bring, what they may need from others, what the state of the art is in the field of the project and should develop a strategy on protection, use and dissemination of the future results. Such activities require

discussions, exchange of information and ideas between the parties.

Dispute resolution: Dispute Resolution Mechanism (DRM) is equally very essential in the legal framework of consortium. Here, parties are to agree beforehand on how disputes are to be resolved when they arise. The agreement should state medium to use to seek redress among members (i.e, use of conventional courts or through Alternative Dispute Resolution (ADR), members that will make up the dispute resolution committee and conditions for choosing arbitrators if there will be any). ADR simply refers to a dispute resolution mechanism that encourages amicable resolution of dispute outside the court rooms using different options such as Arbitration, Mediation, Conciliation and Reconciliation (EMIDA, ERA-NET: Guidelines for a consortium agreement, 2017; BFM Released Meeting, 2013; Ambient Assisted Living (AAL), 2006).

2.2 Ethical considerations on consortium building

The ethical principles to be observed in the study shall be premised on three basic sub-headings: respect the dignity and rights of members, professional competence and responsibility, honesty and integrity in professional relationship.

On respect, consortium members should: have sensible regard for individual member moral, organisational and cultural values; not allow service to members to be diminished by factors such as ownership orientation, religion, race, ethnicity, location, party politics, social standing or class; convey respect for and abide by prevailing consortium mores, social customs, and cultural expectations in their business and professional activities; use language that conveys respect for the dignity of other members (for example, gender-neutral terms) in all written or verbal communication; avoid or refuse to participate in practices which are disrespectful of the legal, civil, or moral rights of other members (Code of Ethics of the Psychological

Society of Ireland (PSI) (2010); McNamara (2008); IFLA (2004)).

On privacy and confidentiality, consortium members should: explore and collect only information which is germane to the purposes of a given investigation or intervention, or which is required by law; take care not to infringe, in research or service activities, on the personally or culturally defined private space of individual member or groups unless clear and appropriate permission is granted to do so; respect the right of members, supervisors, students, or psychologists in training to reasonable personal privacy; take care not to relay, except as required or justified by law, confidential information about others members of consortium to which they have become privy in the course of their professional activities; share confidential information with others only with the informed consent of those involved, or in a manner that the individuals involved cannot be identified, except as required or justified by law, or in circumstances of actual or possible serious physical harm or death; store, handle, transfer and dispose of all records, both written and unwritten (for example, computer files, video tapes, minutes of meetings, foreground, background), in a way that attends to the needs for privacy and security; take all reasonable steps to ensure that records over which they have control remain personally identifiable only as long as is necessary in the interests of those to whom the records refer and/or to the project for which they were collected, or as required by law, and render anonymous or destroy any records under their control that no longer need to be personally identifiable; clarify what measures will be taken to protect confidentiality, and what responsibilities consortium members have for the protection of each other's confidentiality, when engaged in services to or research with individuals in the consortium, other groups or communities outside the consortium; obtain informed consent from all independent and partially dependent members for any consortium services provided to them (Code of Ethics of the Psychological Society of

Ireland (PSI), 2010; McNamara, 2008; IFLA, 2004).

Professional competence and responsibility, consortium members should: strive to ensure and maintain high standards of competence in their work. They shall recognise the boundaries of their particular competencies and the limitations of their expertise. They shall provide only those services and use only those techniques for which they are qualified by education, training or experience. Competence is synonymous with knowledge, skills and ability (Oyewole and Abioye, 2016). Also, consortium members shall be aware of their professional and scientific responsibilities to other members, to the consortium, and to the society in which they work and live. Members shall avoid doing harm and shall be responsible for their own actions, and assure themselves, as far as possible, that their services are not misused.

More specifically, consortium members shall: be aware of how their own experiences, attitudes, culture, beliefs and values influence their interactions with others, and integrate this awareness into all efforts to benefit and not harm others; recognise the boundaries of their competence, and do not exceed these; offer or carry out (without supervision) only those professional activities for which they have established their competence to practise to the benefit of others; take immediate steps to consult or to refer a member/client to a colleague or other appropriate professional, whichever is most likely to result in competent service to the client, if it becomes apparent that they are not competent to deal with a client's problem; avoid delegating professional activities to persons/agents not competent to carry them out to the benefit of others (Code of Ethics of the Psychological Society of Ireland (PSI) (2010); McNamara (2008); IFLA (2004)).

Okerson (2000) noted that a condition for success in consortium is that, within the consortium, members have trust; members must trust one another and themselves well enough in order to

benefit from the cooperation platform. One popular definition of trust cited in most literature is the definition of Mayer, Davis and Schoorman (1995) which opined that trust is the willingness of a party to be vulnerable to the actions of another party based on the expectation that the other will perform a particular action important to the trustee, irrespective of the ability to monitor or control that other party. Evans (2002) sums it up that a successful consortia require time to develop, a high level of trust in one's partner, and a willingness to contribute. Even if there is no effective means of measuring success, the winning issues are the need, the will and the vision of the membership. Usoro (2007) referring to Mayer et al (1995) elaborated factors that influence the creation of integrity-based trust. These include: the independent verification of the trustee's integrity from reputable third parties; perceptions that the trustee holds an acceptable level of moral standards; and demonstration of consistent behavior including congruence between a trustee's actions and words. Usoro (2007) observed that the focus on the alignment between an actor's actions and words is what is defined as behavioural integrity. This is the extent an individual is perceived to walk their talk and vice versa (Simons, 2002). Long-term vision, goals, programming, and objectives will not lead to a successful partnership without the full participation of members. Complete integration of a consortium's goals into each member library's mission is integral to the survival of the partnership.

III. CONCLUSION AND RECOMMENDATION

Consortium is a means by which the objectives of academic libraries can be effectively actualised. However, to ensure success in the cooperation to be formed, intending academic libraries joining the collaboration should fully understand the legal factors required as members. These libraries should agree and be ready to observe all ethical considerations of the consortium to foster healthy coexistence among them. The study therefore

recommends that legal and ethical factors relating to the smooth running and healthy cooperation among academic libraries joining consortium building be known and upheld by all.

REFERENCES

1. Awujoola, O. L. 2018. Institutional, legal and ethical factors as precursors of consortium building readiness among university libraries in South-west, Nigeria. An unpublished seminar paper presented at the Department of Library, Archival and Information Studies, University of Ibadan.
2. Ukwona, S. 2017. Collaborative practices among Public/Private Institutions and National /International Professional Bodies: A paper presented At the Librarians' Registration Council of Nigeria 4th Conference of Certified Librarian in Nigeria held between 5th and 9th November, 2017 at the Public Service Institute of Nigeria, Dutse junction, Kubwa ExpressWay, Abuja.
3. Sacchanand, C. 2012. Building collaboration between library and information science educators and practitioners in Thailand : transcending barriers, creating opportunities. A paper presented at IFLA. <http://conference.ifla.org/ifla78>.
4. Oyewole, O and Abioye, A. 2016. Stemming the tide of plagiarism in thesis writing in Nigerian library schools through policy and competence: Implication for quality assurance. *Proceedings of the Annual National Conference of the Nigerian Association of Library and Information Science Educators (NALISE), 2016*.
5. Ogunleke, I. D. 2015. Awareness and attitude towards professional ethics as determinants of patient information management in selected hospitals in Southwest Nigeria. A master's dissertation submitted to the Department of Library, Archival and Information Studies, University of Ibadan.
6. National Association of School Psychologist: Principles for professional ethics, (PSI). (2010).
7. Murthy, T. A. V. 2002. Resource sharing and consortia for India. Proceeding, IIT Seminar, Kharagpur, Feb. 2002: pp.14-15.
8. Mohammed, A. 2015. Collaboration among library and information science schools for effective teaching in the Knowledge society in Nigeria: proposed Model.
9. *Bayero Journal of Library and Information Science* 2.1: 1-66.
10. McNamara, k. 2008. Best practices in the application of professional ethics. In A. Thomas and J. Grimes (Eds), Best practices in school psychology (pp. 1933-1941). Bethesda, MD: National Association of School Psychologist.
11. Mayer, R. C, Davis, J. H and Schoorman, F. D. 1995. An integrative model of organisational trust. *The Academy of Management Review* 20.3: 709-734
12. Jelena, Božović. 2007. Business Ethics in Banking. *Journal Series: Economics and Organization* 4.2: 173 – 182.
13. Ike-Mbofung, U. I. 2015. Self-management, legal and ethical issues as determinants of information service delivery among librarians in federal university libraries in Nigeria. A PhD thesis submitted to the Department of Library, Archival and Information Studies, University of Ibadan.
14. Idolohor, E. J. 2010. Banking Frauds in Nigeria: Underlying Causes, Effect and Possible Remedies, *African Journal of Accounting, Economics, Finance and Banking Research*, 6.6: 62-80.
15. International Federation of Library Association (IFLA). 2004. IFLA and professional ethics.
16. Hulagabali, Santosh. C. 2012. Understanding the Library Consortium to Harness the Teaching, Research and Publication Activities. *Administration* 8: 15-29.
17. Evans, G. E. 2002. Management issues of co-operative ventures and consortia in the USA. Partone. *Library Management*, 23.4 & 5.
18. Etim, F. E. 2006. Resource sharing in the digital age: Prospects and problems in African

- universities,” *Library Philosophy and Practice* 9/1: 1-5 (2006). <http://unllib.unl.edu/LPP/etim.pdf>
19. Erundu, E. A., Sharland, A., and Okpara, J. O. 2004. Corporate Ethics in Nigeria: A Test of the Concept of an Ethical Climate. *Journal of Business Ethics* 51.1: 124-132.
 20. Bedi, S and Sharma. K. 2008. Library Consortia: A Step forward the Information Society, Electronic address: Panjab University, Chandigarh dlist.sir.arizona.edu/2289/01/Shalu_Bedi_and_Kiran_sharma_LIBRARY_CONSORTIA.
 21. American History Dictionary of the English Language. 2000. 4th ed. Boston: Houghton Mifflin Company.
 22. Ali, H., Owoeye, J. E., and Anasi, S. N. I. 2010. Resource sharing among Law Libraries: *An imperative for legal research and the administration of justice in Nigeria. Library Philosophy and Practice* 2010 (July).
 23. Haslinda Abdullah and Benedict, Valentine. 2009. Fundamental and ethics theories of corporate governance. *Middle Eastern Finance and Economics* Issue 4, p. 6.
 24. Nwalo, K. I. N. and Ogunniyi, S.O. 2012. Networking of academic libraries in Ondo State, Nigeria. *A paper presented at the 50th National Conference and Annual General Meeting of the NLA held from 15th-19th July, 2012.*



Scan to know paper details and
author's profile

Fine-Structure Constant as Pure Geometric Number among Physical Background

Mei ZH

Qingdao University of Science and Technology

ABSTRACT

According to B. Feng's theory, the Fine-Structure Constant is theoretically deduced as, $\alpha^{-1} = \frac{64}{3} 2\pi k^{-1}$
=137.0359970, an accurate theoretical value.

Keywords: fine-structure constant, four- dimensional spherical space, space-time manifold, variable mode
effect.

Classification: FOR code:100306

Language: English



London
Journals Press

LJP Copyright ID: 925646
Print ISSN: 2631-8490
Online ISSN: 2631-8504

London Journal of Research in Science: Natural and Formal

Volume 19 | Issue 2 | Compilation 1.0



© 2019, Mei ZH. This is a research/review paper, distributed under the terms of the Creative Commons Attribution-Noncommercial 4.0 Unported License <http://creativecommons.org/licenses/by-nc/4.0/>), permitting all noncommercial use, distribution, and reproduction in any medium, provided the original work is properly cited.

Fine-Structure Constant as Pure Geometric Number among Physical Background

Mei ZH

ABSTRACT

According to B. Feng's theory, the Fine-Structure Constant is theoretically deducted as, $\alpha^{-1} = \frac{64}{3} 2\pi k^{-1} = 137.0359970$, an accurate theoretical value.

Keywords: fine-structure constant, four-dimensional spherical space, space-time manifold, variable mode effect.

Author: College of Chemistry and Molecular Engineering, Qingdao University of Science and Technology, Zhengzhou Road, Qingdao 266042, China.

I. INTRODUCTION

Fine-structure constant (α^{-1}) is a well-known natural constant in physics. It was beginning with an experimental discovery of fine spectrum of light (Michelson, 1887) and was first defined and theoretically explained by Sommerfeld in 1916. The measuring method by using Quantum Hall Effect has been recognized as advanced; the recent accurate value recommended by CODATA in 2014 is as 137.035999139(31).

Fine-structure constant is a combined dimensionless constant and appears in many physical occasions. Many physicists pay much attention to it mainly because of its dimensionless. Though Sommerfeld has given it a good explanation, still the physicists continuing their work for searching its deeper reason: wondering why the "hand of God" wrote down such a mystery non-integer number?

II. ANALYSIS

Believing it to be a mathematical combination of integer numbers and mathematical constant, the

guess works appeared uninterruptedly ever since, as Wyler's $(9/16\pi^3)(\pi/5!)^{1/4} = 1/137.036$, Eddington's $(162 - 16)/2 + 16 = 136$, and others as $(9/8\pi^4)(\pi^5/2^45!)^{1/4} = 1/137.036082$, $(1 - 1/(30 \times 127))/137 = 1/137.035967$, $\cos(\pi/137)/137 = 1/137.036028$ and $29\cos(\pi/137)\tan(\pi/(137 \times 29))/\pi = 1/137.035999787$ etc. All of these are said to be mathematical games and can't give out any information of physical meaning.

The actual determined value would depart from its original theoretical one because of the influences from the measuring method, measuring interaction and relativistic effect. Here, the original theoretical value would be more effective than that of actual to us for revealing the essential law of things, like that in dealing with the gas state function; where the ideal gas is more attractive to us.

III. DEDUCTION

According to Sommerfeld's definition, the original theoretical form and value of α^{-1} is as follows:

$$\alpha^{-1} = \frac{c}{v_e} = \frac{2\varepsilon_0 hc}{e^2} \dots\dots\dots (1)$$

$$= \frac{2 \times 8.85418781871 \times 10^{-12} \times 6.626069934 \times 10^{-34} \times 2.99792457982 \times 10^8}{(1.6021766208 \times 10^{-19})^2}$$

$$= 137.0359970 \dots\dots\dots (1.1)$$

According to recent proposed B. Feng's theory [1], the charge value of an elementary particle can be expressed by other common physical constants. The deduction steps were as following:

Supposing the Universe to be a four-dimensional spherical space (five-dimensional Euclid space), its projection in four-dimensional Euclid space would produce *variable mode* effect.

Because there is the following relationship between the surface area (S) and volume (V) of the n -dimensional sphere:

$$\frac{V_n}{S_{n-1}} = \frac{R}{n}, \text{ and } \frac{S_{n+1}}{V_n} = 2\pi R$$

So, the area of four-dimensional spherical space (S_4) and the volume of four-dimensional Euclid space (V_4) is $S_4 = 8\pi^2 R^4/3$ and $V_4 = \pi^2 r^4/2$ respectively. Where the radius R and r has a variable mode effect, their relation is as

$$R = \sqrt{\Omega^2 + (ct)^2} = \sqrt{r^2 + r^2} = \sqrt{2} r$$

It shows that the radius variable mode coefficient is $\sqrt{2}$.

The energy ratio of four-dimensional spherical space (E_S) to four-dimensional Euclid space (E_E) is equal to the corresponding area-volume ratio, we have

$$E_S = \frac{8\pi^2 R^4 / 3}{\pi^2 r^4 / 2} E_E = \frac{8 \times 2 \times (\sqrt{2})^4}{3} E_E = \frac{64}{3} E_E \dots\dots\dots (2)$$

It shows the energy variable mode coefficient is $64/3$.

Though the Universe is a four-dimensional spherical space, and we right live in such a complex space, however, in a condition of low velocity world, we more look like living in a simple

$$e^2 = \frac{3}{64\pi} \frac{h}{c\mu_0} \dots\dots\dots (5)$$

$$= \frac{3}{64\pi} \frac{6.626069934 \times 10^{-34}}{2.99792457982 \times 10^8 \times 4\pi \times 10^{-7}} = \frac{3}{256\pi^2} \frac{6.626069934 \times 10^{-35}}{2.99792457982} = 2.624320399888 \times 10^{-38}$$

$$e = \pm 1.6199754319 \times 10^{-19} \text{ C}$$

However, the measured charge of an electron is $1.6021766208 \times 10^{-19} \text{ C}$. In such a case, append a fitting factor k in (5), and in order to make them equal, let $k = 0.9781465420$, thus

$$e^2 = \frac{3}{64\pi} \frac{hk}{c\mu_0} = (1.6021766208 \times 10^{-19})^2 \dots\dots\dots (6)$$

Substituting (1) with (6), we have

four-dimensional Euclidean space. The work energy we do can only belong to the four-dimensional Euclid space's (E_E). In classical physics, the Euclid energy (E_E) can be calculated based on Biot-Savart Law and Lorenz force (F) Law of moving charge (e) in magnetic field intensity (B), we have

$$E_E = l \times F = 2\pi r F = 2\pi r \times ecB = 2\pi r \times ec \frac{\mu_0 ec}{4\pi r^2}, \text{ (where, } l \text{ is}$$

the charge moving distance in a circle) i.e.

$$E_E = \frac{\mu_0 e^2 c^2}{2r} \dots\dots\dots (3)$$

As elementary particles, electron and proton are indeed the confined movement of light (along the time axis) [2, 3], their energy belongs to four-dimensional spherical space (E_S). The classical Euclidean energy E_E in (3) ought to be converted by (2). Combining (2) and (3), we have

$$E_S = \frac{64}{3} \frac{\mu_0 e^2 c^2}{2r} \text{ . As frequency } (\nu) \text{ has a relation of}$$

$$\nu = \frac{c}{2\pi r}, \text{ we can rewrite } E_S \text{ as}$$

$$E_S = \frac{64}{3} \pi \mu_0 e^2 c \nu \dots\dots\dots (4)$$

Because energy has the form as $E = h\nu$, we have

$$h\nu = \frac{64}{3} \pi \mu_0 e^2 c \nu, \quad h = \frac{64}{3} \pi \mu_0 e^2 c,$$

$$\alpha^{-1} = \frac{2\varepsilon_0 hc}{e^2} = \frac{2\varepsilon_0 hc}{3} \frac{hk}{64\pi \mu_0 c} = \frac{2\varepsilon_0 hc \times 64\pi \mu_0 c}{3h} = \frac{64}{3} 2\pi k^{-1} \varepsilon_0 \mu_0 c^2,$$

as $c^2 = \frac{1}{\varepsilon_0 \mu_0}$, we finally obtained

$$\alpha^{-1} = \frac{64}{3} 2\pi k^{-1} \dots\dots\dots (7)$$

$$= \frac{64}{3} 2\pi \times \frac{1}{0.9781465420}$$

$$= 137.0359970$$

That's just the exact value that calculated theoretically in (1.1).

IV. DISCUSSION

From the expression in (7), one can see a perfect geometric character of α^{-1} . Where $64/3$ is a geometric energy variable mode coefficient, 2π the common circumference ratio. And k is also a geometric circumference; outwardly, it plays as a fitting number in (6), however, it comes from a not considered factor in the theoretical deduction of electric charge in (5). The not considered factor would be the curved space coefficient, because, in the process of theoretical deduction in (2)-(5), we treat the space as a plane Euclid's; nevertheless, the mass density of electron is as high as 1.36512×10^{10} g/cm³, where the curved space factor can't be neglected. In this way, the adding of k in (6) is necessary and reasonable, as a treating method which has ever been used in our previous work [4] when calculated the mass spectrum of elementary particles, where the same meaning of k was given a fitting number of 0.970624. They look almost to be equal.

From above theoretical deduction process, obviously, it shows us a strong physical background of α^{-1} rather than a mathematical game.

Another thing is that, to our surprising, the mystery number of α^{-1} is just the radius of proton which we predicted in literature [5].

V. CONCLUSION

α^{-1} is equal to $\frac{64}{3}2\pi k^{-1}$. It consists of pure geometric parameters of $64/3$, 2π and spatial bending factor k .

REFERENCES

1. Feng B. The topological analysis of material structure. Journal of Wuyi University, 2013, 27(1):42-49.
2. Mei ZH, Mei SY. Mass the Confined Movement of Energy. Journal of Modern Physics, 2017, 8:923-925.
3. Mei ZH. B. Feng's Theory (Part II): The Origin of Charge and the Unified Field Theory-Going on Kaluza-Klein's. J Phys Astron, 2018, 6 (1):131-140.
4. Mei ZH. B. Feng's Theory: The Prediction of Mass Spectrum of Elementary Particles and the Confidence of at Least 4-D Space-Time (Part I), Journal of Physics & Astronomy, 2017, 5(3):126-132.
5. Mei ZH, Shi J. B. Feng's Theory (Part III): Neutron Model and Nuclei Force Mechanism. Journal of Physics & Astronomy, 2018, 6(1):143-149.

This page is intentionally left blank



Scan to know paper details and
author's profile

Temperature Dependence of Static Dielectric Constant of Lophiralanceolata (Echinacea) Oil

Najoji, S. David & Yerima, J. Benson

The Federal Polytechnic Damaturu

ABSTRACT

Using parallel plates capacitor (10 cm × 10 cm) at the mains frequency (50 Hz), the static dielectric constant of lophiralanceolata oil (LLO) was measured at different temperatures. The results show that the static dielectric constant decreases with increasing temperature according to the Clausius-Mosotti equation for polar dielectrics. From dielectric measurements, some properties of LLO which include total polarizability, permanent dipole moment and molar refraction of the molecule were determined. Our results show that LLO is a polar dielectric which is an important indicator of oil quality. Even though our technique is cheap, simple and agrees with existing theories, there are several sophisticated methods for more accurate measurements.

Keywords: static dielectric constant, Lophiralanceolata oil, Temperature, permanent dipole moment, total polarizability, molar refraction.

Classification: FOR code:069999

Language: English



London
Journals Press

LJP Copyright ID: 925647
Print ISSN: 2631-8490
Online ISSN: 2631-8504

London Journal of Research in Science: Natural and Formal

Volume 19 | Issue 2 | Compilation 1.0



© 2019. Najoji, S. David & Yerima, J. Benson. This is a research/review paper, distributed under the terms of the Creative Commons Attribution-Noncommercial 4.0 Unported License <http://creativecommons.org/licenses/by-nc/4.0/>, permitting all noncommercial use, distribution, and reproduction in any medium, provided the original work is properly cited.

Temperature Dependence of Static Dielectric Constant of Lophiralanceolata (Echinacea) Oil

Najoji, S. David^α & Yerima, J. Benson^σ

ABSTRACT

Using parallel plates capacitor (10 cm × 10 cm) at the mains frequency (50 Hz), the static dielectric constant of lophiralanceolata oil (LLO) was measured at different temperatures. The results show that the static dielectric constant decreases with increasing temperature according to the Clausius-Mosotti equation for polar dielectrics. From dielectric measurements, some properties of LLO which include total polarizability, permanent dipole moment and molar refraction of the molecule were determined. Our results show that LLO is a polar dielectric which is an important indicator of oil quality. Even though our technique is cheap, simple and agrees with existing theories, there are several sophisticated methods for more accurate measurements.

Keywords: static dielectric constant, Lophiralanceolata oil, Temperature, permanent dipole moment, total polarizability, molar refraction.

Author α: Department of Basic Science, School of General and Remedial Studies, Federal Polytechnic P.M.B. 1006, Damaturu, Yobe State, Nigeria.

σ: Department of Physics, School of Physical Sciences, Moddibo Adama University of Technology P.M.B 2076 Yola, Adamawa State, Nigeria.

I. INTRODUCTION

Lipids or fats are naturally occurring inorganic or organic substances that are soluble in organic solvents but not soluble in water. Most fats containing organic materials are made up of carbon, hydrogen, oxygen and some elements like phosphorus. Chemically, fats are carboxylic acids (esters) derived from the single alcohol, glycerol,

and are known as glycerides. Liquid fats are referred to as oils. Oils are mostly extracted from living animals and plants as well as their dead remains in rock underground. The physical and chemical properties of oil depend on its molecular weight (atomic elements present) and the arrangement of atoms in the molecules or molecules themselves that constitute the acid chains of the oil (Yerima, 1988; Eromosele and Eromosele, 1993). A host of authors have studied both Physical and chemical properties of oils (Eromosele et al., 1994; Eromosele and Pascal, 2002, Carey, 1998; Manji et al. 2006; Nkafamiya et al., 2007; Miller et al., 2005). Oils are used as fuel (kerosene, gasoline), lubricants (in moving parts of machines/engines to reduce friction and heat), cream (body and hair), medicinal purposes (e.g. shear butter, lophiralanceolata, cobra, etc. oils are used to cure diseases like aromantism, rashes, bone fracture and many other diseases), in cooking (vegetable oils), in making paints/soap and as dielectrics in capacitors to mention a few (Carey and Hayzen, 2001).

A dielectric material or an insulator has no free electric charges (electrons) under normal circumstances. This does not mean that they cannot modify the electric field into which they are introduced. In other words, a dielectric is one that has poor conductivity, but an ability to hold a charge with an applied electric field. Examples of dielectrics include air, oil, paper, wax, ceramic, mica, and so on. In fact the most important and interesting electrical property of a dielectric is its ability to become polarized under the action of an external electric field. The atoms and molecules of dielectrics are influenced by an external electric field and hence the positive particles are pushed in the direction of the field while the negative

particles in the opposite direction from their equilibrium position. Hence dipoles are developed and they produce a field of their own. The process of producing electric dipoles out of neutral atoms and molecules is referred to as polarization. A dipole is an entity in which equal positive and negative charges are separated by a small distance. In this case, the dipole moment has magnitude which is the product of charge and separation between the charges represented by a vector pointing from the negative charge in the direction of the positive charge. The units of the dipole moment are the Debye's (1 Debye = 3.33×10^{-30} Coulomb-metre). The dielectrics are mostly useful engineering materials. Their extensive applications as insulators and capacitors as well as their properties can predetermine the electrical performance and quality of such devices (Miller et al., 2005). The first fundamental experimental result discovered by Faraday showed that the capacitance of a capacitor is increased if the space between the conducting parallel plates is filled with a dielectric material (Yerima, 1988). If C_0 is the capacitance of the capacitor with the space between the conductors evacuated and C its capacitance when the space is filled with a dielectric, then the ratio $C/C_0 = k$ is called relative permittivity or dielectric constant which is independent of the shape or dimensions of the conductors and is solely a characteristic of the dielectric medium (Serway, 1996). The dielectric constant is a measure of its ability to transmit electrical potential energy. In electrical systems such as capacitors, the effectiveness of dielectrics is measured by their ability to store electrical energy. For fixed potential difference between the plates of a capacitor, the charge on the capacitor and its capacitance increase by a factor k while for fixed charge, the electric field intensity and potential difference between the plates decrease by $1/k$ of their original values before the dielectric is introduced between the plates (Yerima, 1988). The permittivity of the dielectric medium is defined as $\epsilon = \epsilon_0 k$ where $\epsilon_0 = 8.854 \times 10^{-12}$ Fm⁻¹ is an electric constant representing the permittivity of free space or

vacuum. In another vein, the dielectric constant is a simple number, that is, the ratio of the speed of an electric field in a vacuum or air to the speed of the electric field in a material. The dielectric constant of a material is a directly measurable quantity which expresses on a macroscopic scale the overall result of the interaction which occurs on a microscopic scale between an externally applied electric field and the atoms or molecules of the material. In a nutshell, it is a macroscopic quantity that measures how effective an electric field is in polarizing the material.

When the dielectric constant of oil is measured, changes in the dielectric constant of the oil may be due to the presence of contaminants (water, particles, etc.) or changes in the chemistry of the oil (additive depletion or oxidation). In general, the value of the dielectric varies with the frequency of the applied field. This paper discusses static dielectric constant that is below electric field frequencies of 10⁶ Hz (Carey, 1998; Carey and Hayzen, 2001). Dielectric constants at these frequencies are called static because the dielectric constant of materials shows virtually no frequency dependence in this frequency region. Temperature affects the value of the dielectric constant although the effects are relatively small (0.05 %) or hydrocarbons lubrication oils (Carey and Hayzen, 2001). The density of the oil also influences the dependence of the dielectric constant on temperature- the less dense an oil, the fewer number of oil molecules per unit volume. A smaller number of molecules per unit volume means that there is less interaction with the electric fields and therefore a decrease in the dielectric constant. As the temperature increases, the density decreases and hence the dielectric constant of the oil also decreases. Other things that will change the dielectric constant of oil include an increase in viscosity, changes in acid number or base number and additive depletion or decrease in viscosity caused by addition of less dense oil will result into decrease in dielectric constant (Manji et al, 2007).

It is easy to distinguish different classes of oil by measuring the dielectric constant. The only other

common technology capable of this is infrared spectroscopy (Carey and Hayzen, 2001). However, this method typically requires an expensive instrument and expert interpretation. By contrast, measuring the dielectric constants using capacitors offers a quick, simple, low cost alternative to permit the differentiation between different classes of oil.

In this study, the parallel plates capacitor technique is employed and the dielectric constant of interest is one of the Nigerian vegetable oils known as lophiralanceolata oil (LLO). This oil is extracted from the seed of Lophiralanceolata plant (ochracea) popularly known in northern part of Nigeria in “Hausa language” as “Namijinkadanya”. Previous studies have shown that it has some medicinal (David, 2008) and biomass potentials (Samuel and Maimuna, 2007) and its present use as lubricant (David, 2008) in sewing machines in Mapeo village in Ganye Local Government, Adamawa state, Nigeria. In this paper, our chief interest is to investigate the potential of (LLO) as dielectric in capacitors.

II. THEORY

The charge on the plates of a parallel plate capacitor connected to a power supply kept at constant voltage V with air between its plates is $Q_{\text{air}} = C_{\text{air}}V$ and the charge with oil between its plates is $Q_{\text{oil}} = C_{\text{oil}}V$ where C_{air} and C_{oil} respectively are the capacities of the capacitor with air and oil between its plates. Taking the ratio of the two charges and noting that the dielectric constant, k of a dielectric between the plates of a parallel plate capacitor is defined as the ratio of the capacity of the capacitor with oil as dielectric between its plates to that with air as dielectric. Thus, from the two equations, we can see that $k = Q_{\text{oil}}/Q_{\text{air}}$. Since charge is proportional to current or deflection in a galvanometer then this equation becomes $k = \theta_{\text{oil}}/\theta_{\text{air}}$. Using very sensitive galvanometer this method has been successfully employed to measure the dielectric constant of lophiralanceolata oil at various temperatures. It is worthy to note that the theory is cheaper and

simpler compared to other methods such bridge, frequency, infrared spectroscopy and so on.

III. METHOD

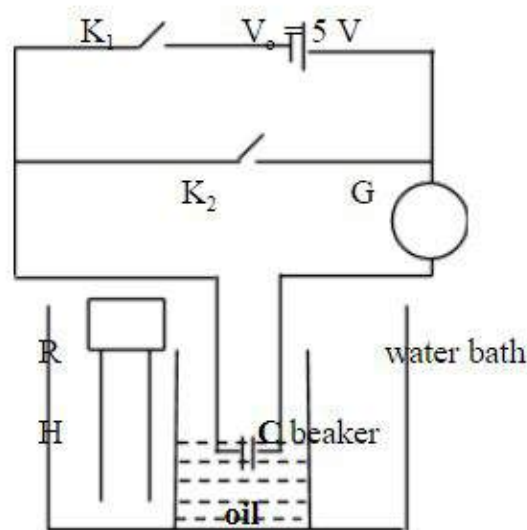


Fig. 1: Schematic diagram for measuring static dielectric constant of LLO

First, a parallel plate capacitor of dimensions $10\text{ cm} \times 10\text{ cm}$ and plates separation of 1 mm was constructed. With air as dielectric, when K_1 was closed and K_2 opened, the capacitor C was charged to maximum voltage $V_0 = 5\text{ V}$. When K_1 was opened and K_2 closed, the maximum deflection θ_{air} on the galvanometer was recorded. The space between the plates of the capacitor was completely filled with lophiralanceolata oil (LLO). The capacitor was gently immersed in water in the water bath with its open end just slightly above the water meniscus in the water bath. The capacitor with oil between its plates was immersed in the water in the bath was heated to a constant temperature by means of an electric heater (H) and stirrer which are elements of the automatic bimetallic temperature regulator R (PHYWE 08482.93, Nr 986, 220V 50 Hz 3.5A). With LLO as dielectric, the procedure of measuring maximum deflection θ_{oil} was repeated at various temperatures with the capacitor dipped in the water bath in such a way its open end was slightly above the water surface (Fig.1). The expression for dielectric constant $k = \theta_{\text{oil}}/\theta_{\text{air}}$ as developed earlier in the theory was used to

calculate the static dielectric constant of LLO at the mains frequency (50 Hz) at various temperatures (Table 1). The variation of the capacitance of a parallel plate capacitor with temperature up to 60 K above room temperature

with air as dielectric is assumed to be negligible (Yerima, 1988). In the light of this, the value of $\theta_{\text{air}} = 1.2$ determined at room temperature 293 K was kept constant in the calculation of the values of k in the temperature range 293-353 K (Table 1).

III. RESULTS AND DISCUSSION

Table 1: Dielectric constant of LLO, ($\theta_{\text{air}} = 1.2$; $V_{\text{air}} = 5 \text{ V}$)

T(K)	θ_{oil}	$k = \theta_{\text{oil}}/\theta_{\text{air}}$	$n = \sqrt{k}$
293	4.0	3.33	1.824
298	3.8	3.17	1.780
303	3.5	2.92	1.708
308	3.2	2.67	1.634
313	3.0	2.50	1.581
323	2.9	2.40	1.549
333	2.8	2.33	1.526
343	2.6	2.17	1.472
353	2.5	2.08	1.442

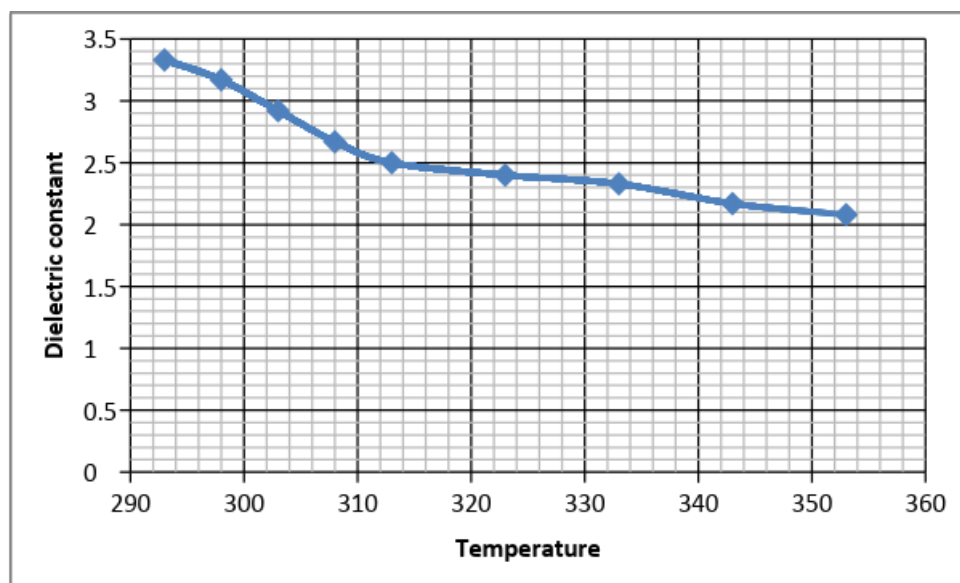


Fig. 2: Variation of dielectric constant of LLO with temperature

The values of dielectric constant, k of LLO were determined at various temperatures (Table 1). Fig.2 shows that the dielectric constant of LLO decreases with increasing temperature T in the range 293- 353 K. On heating, oils are known to undergo thermal degradation and decomposition as a result of some secondary reactions that produce polar compounds such as free fatty acid, hydroxyl compounds, diperoxides, and mono- and di-triglycerides which decreases k with T (Manji et al, 2007; Hwang et al, 1994). Also the decrease in

k with T may be attributed to larger polarizable hydrocarbon molecules in LLO just like most seed (groundnut, palm, peanut, sesame, cotton, sunflower, corn) oils reported to contain fatty acids and mainly 16-18 carbon atoms (Carey and Hayzen, 2001). The value of dielectric constant (3.33 ± 0.48) determined at room temperature is higher than that of previous workers (2.14) (Samuel and Maimuna, 2007). Even though Samuel and Maimuna (2007) did give error in their result, the difference may be attributed to

the age and amount of slurry particles present depending on the different methods of extraction. The amount of slurry particles present is expected

to affect the density and hence the dielectric constant.

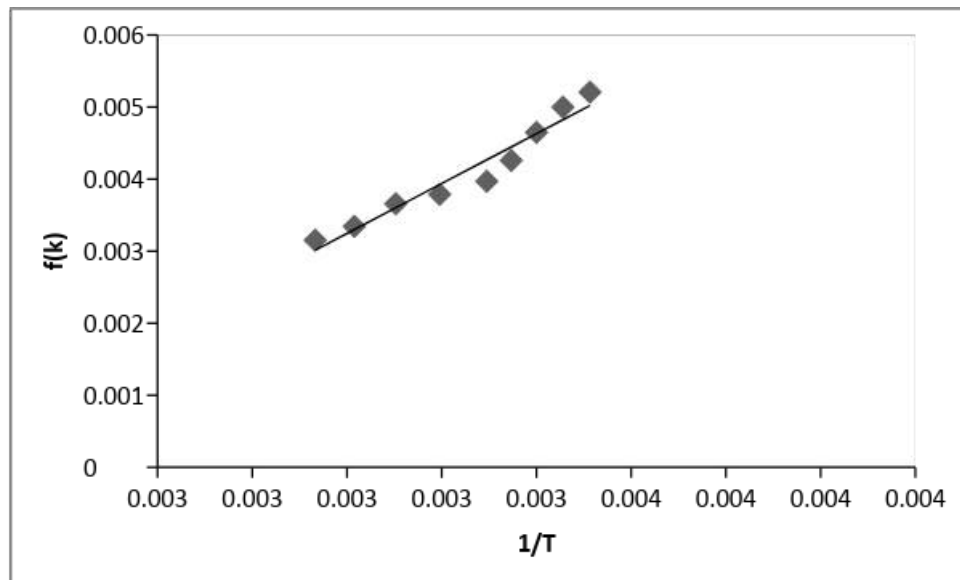


Fig. 3: Variation of f(k) with 1/T

Figure 3 represents the plot of the function $f(k) = \left(\frac{k-1}{k+2}\right)V_m$ against $1/T$ according to the Clausius-Mosotti or modified Debye equation

$$\left(\frac{k-1}{k+2}\right)V_m = a + \frac{b}{T}$$

where V_m , a and b are constants

with $a = \frac{\alpha N_A}{3\epsilon_o}$, $b = \frac{N_A \mu_m^2}{9\epsilon_o k_B}$. Applying the Clausius-Mosotti equation to LLO and using the constant $V_m = \text{molar volume of LLO} = 11.91 \times 10^{-3} \text{ m}^3$ (David, 2008), $N_A = \text{Avogadro's number} = 6.02 \times 10^{23}$, $\epsilon_o = \text{permittivity of free space} = 8.854 \times 10^{-12} \text{ Fm}^{-1}$ and $k_B = \text{Boltzmann's constant} = 1.38 \times 10^{-23} \text{ JK}^{-1}$, the quantities $\alpha = \text{total polarizability}$ and $\mu_m = \text{permanent dipole moment}$ using least square were calculated to be $-1.32 \times 10^{-35} \text{ Fm}^2$ and $79.5 \times 10^{-30} \text{ Cm}$ from the intercept and slope respectively.

The total polarization P is equal to the sum of induced polarization P_i (atom-polarization P_a due to nuclei distortion + electron-polarization P_e due

to electron distortion) plus orientation polarization P_o i.e. $P = P_a + P_e + P_o = P_i + P_o$. Maxwell showed that for the same electromagnetic wave, the refractive index (n) of a medium is related to its dielectric constant (k) by the equation $k = n^2$. Therefore, the total polarization $P = \left(\frac{k-1}{k+2}\right)V_m$ appears replaceable by

the molar refraction $R_m = \left(\frac{n^2-1}{n^2+2}\right)V_m$. But this is not strictly so. The refractive index is measured with visible radiations of higher frequency ($\sim 10^{14} \text{ Hz}$) whereas the static dielectric constant is measured with long waves ($< 10^2 \text{ Hz}$). The refractive index changes somewhat with wavelength. The correction for refractive index (n) for lower frequency can be obtained with the

empirical Cauchy formula $n = n_\infty + \frac{a}{\lambda^2}$ (Rakshit, 1997) where $n = \text{refractive index at wavelength } \lambda$ and n_∞ at very high wavelengths; a is a constant whose value may be ascertained from two

measurements of n at known frequencies in the visible region.

In refraction only electrons are affected by the radiation. Even when corrected for long waves the refractive index gives the effect of the long waves on the electrons only. The nuclei remain unchanged. Thus, the electron-polarization equals

the molar refraction $R_m = \left(\frac{n_e^2 - 1}{n_e^2 + 2} \right) V_m$. (Rakshit, 1997). Substituting the values $V_m = 11.91 \times 10^{-3} \text{ m}^3$ and $n = 1.463$ obtained by David (2008) gives $R_m = 3.28 \times 10^{-3} \text{ m}^3$ at 30°C .

IV. CONCLUSION

At various temperatures the static dielectric constant of LLO was determined using AC source operated at the mains frequency (50 Hz). The results show that the static dielectric constant decreases with increasing temperature obeying the Clausius-Mosotti relation for polar dielectrics. Using the values of measured dielectric constant, other properties of LLO such as total polarizability, permanent dipole moment and molar refraction (electron-polarization) were deduced. However, there is still room to improve on the accuracy of our results more especially if the empirical Cauchy formula for correction for the refractive index for lower frequency is employed. We also observed that LLO has potentials to be used as coolant in refrigerators and rheostats, inhibitor of oxidation and corrosion, lubricant in non-vehicle engines and dielectrics in capacitors.

REFERENCES

1. S. J. Miller; S. Shan and G. P. Hoffman (2005) Conversion of waste plastic to lubricating base oil. *Energy and Fuel*. Vol 4, 887-896.
2. R. A. Serway (1996) *Physics for Scientist and Engineers*, 4th edition 2nd printing, Saunders College Publishing, 27.
3. J. B. Yerima (1988) Some physical properties of groundnut oil, palm oil and coconut water and their temperature dependence, B. Sc. Project University of Maiduguri.
4. Y. M. David (2008) Some physical properties of lophiralanceolata oil and their temperature dependence, B. Tech. Project submitted to Federal University of Technology Yola.
5. A. J. Manji, B. A. Aliyu; I.I.Nkafamiya and U.U.Moddibo (2007) Studies on the degradation of cotton seed oil used for shallow frying, *Nigerian Journal of Exptal and applied Biology*, 8(1), 131-136.
6. A. J. Manji, B. A. Aliyu and I.I.Nkafamiya (2006) Degradation of groundnut oil used for shallow frying, *J. Chem. Soc. Nigeria*, vol 31 (1&2), 22-22.
7. I.I.Nkafamiya; B. A. Aliyu; A. J. Manji and U.U.Modibbo (2007) Dehradation properties of wild *Adansoniadigitata* (baobab and *Prosopsis Africana*(Lughu) oils on storage. *African J. of Biotech.* Vo l6(6), 751-755.
8. J. C. Eromosele and C. O.Eromosele (1993) Studies on the chemical composition and physio-chemical properties of seeds of some wild plant. *Food for human nutrition*. 43 Kluwer Academic Publishers, Netherlands, 251-258.
9. J. C. Eromosele; C. O. Eromosele, and T. O. Komolafe (1994) Characterization of oils and chemical analysis of seeds of wild plant. *Food for human nutrition*. 46 Kluwer Academic Publishers, Netherlands 38-46.
10. C. O. Eromoseleand N. H. Pascal (2002) Characterization and viscosity parameters of seed oils from wild plants. *Sci. Dir. J of Bioresource Tech.* 818.
11. Y. G. Hwang; U. K-G Kang and M. Seang (1994) Relationship between physical and chemical properties of frying vegetable oils, *HangukSilklyonHakhoechi* 23 (4): 654-659
12. P. C. Rakshit (1997) *Physical Chemistry*, 4th reprint, Calcutta: P. M. Bagchi, Modern Book Agency Private Limited, 88.
13. A. A. Carey and A. J. Hayzen (2001) *The Dielectric Constant and Oil Analysis*, CSI, Practicing oil analysis Magazine. Lean Manufacturing, 2-4.
14. A. A. Carey(1998) *The Dielectric Constant of Lubrication Oils*. Computational Systems

Incorporated, 835 Innovation Drive, TN37932
(423) 675-2110.

15. S. O. Pillai (2005) Solid state Physics, 6th edition, New Age International (p) Publishers, New Delhi, 625-653.
16. F. Samuel and K. Maimuna (2007) Biomass potential of LophiraLanceolata Fruit as renewable energy source, African Journal of Biotechnolohy, vol (7) 3, 308-310.